

The Synthesis of Neutral Metal Complexes That Partition to the Membranes of Lipid
Vesicles

by

Dongman Xi

A thesis submitted in partial fulfillment of the requirements for the degree of

Master of Science

Department of Chemistry
University of Alberta

© Dongman Xi, 2022

Abstract

Life relies on membranes, electron transfer reactions and proton-gradients. To better understand if electron transfer within and proton gradients across a lipid membrane could be achieved with simple, prebiotically plausible components, we synthesized prebiotically plausible neutral metal complexes which are redox active. These metal complexes partitioned to the membranes of lipid vesicles and should be capable of participating in an electron transport chain.

Here, different thiol ligands and imidazole ligands were first chosen and used to synthesize Co (II) complexes in water-octanol mixtures. According to the UV-Vis spectra of different Co (II) complex in octanol, the logic and method of octanol-soluble metal complex synthesis was obtained and then applied to the synthesis of Fe (II) complexes. The UV-Vis spectra indicated that octanol soluble Fe (II)-N-Acetyl-L-cysteine-1-butylimidazole complex was successfully synthesized. Subsequently, such complexes were synthesized in the membranes of phospholipid vesicles and detected by ^{31}P NMR spectra. Increased linewidths indicated that Fe (II) complexes successfully migrated to the membranes of phospholipid vesicles.

Acknowledgement

First and foremost, I would like to thank my supervisor Sheref S. Mansy that allowed me to explore the incredible field of the research on the origin of life. I am very grateful for his patience and valuable advice and suggestions during the research.

I want to thank the Dr. Julianne M. Gibbs and Dr. Matthew Macauley for their time and suggestion for my research.

Other thanks go to all the past and present Mansy Lab members, a group of friendly people, who gave me many helps and provided me a great atmosphere for doing research. Many thanks to Dr. Shibaji Basak, and Dr. Serge Nader, Daniele Rossetto, Luca Valer, and Anju, their precious help and suggestions gave me many inspirations.

I also want to thank Mark Miskolzie for his help with ^{31}P NMR spectroscopy.

Finally, I must express my gratitude to my family and friends, their love and support give me strength and courage throughout the years of graduate study.

Table of Contents

Chapter 1.....	1
Introduction.....	1
1.1 The Origins of Life	1
1.2 Lipid and membrane forming compound	3
1.3 Metal in the prebiotic world.....	4
1.4 Cobalt complex used as a spectroscopic probe.....	5
Chapter 2.....	7
Synthesis and characterization of Cobalt complex.....	7
2.1 Introduction	7
2.2 Synthesis and characterization of Co (II)-thiol and Co (II)- imidazole complex	8
2.2.1 Experimental plan.....	8
2.2.2 Co (II)- β -mercaptoethanol complex	8
2.2.3 Co (II)-DTT complex	10
2.2.4 Co (II)-N-Acetyl-L-cysteine methyl ester complex	10
2.2.5 Co (II)-imidazole complex	11
2.3 Synthesize and characterization of Co (II)-thiol-imidazole complex	12
2.3.1 Experimental plan.....	12
2.3.2 Co (II)- β -mercaptoethanol-imidazole complex and Co (II)-N- Acetyl-L-cysteine methyl ester-imidazole complex.....	12
2.4 Synthesis and characterization of Co (II)-imidazole-thiol complex in the mixture of octanol and HEPES	14
2.4.1 Experimental plan.....	14
2.4.2 Experimental Results	15
2.4.3 Discussion.....	27
2.5 Binding affinity of thiol-containing ligands and imidazole ligands to Co (II).....	28
2.5.1 Experimental plan.....	28
2.5.2 Experimental results	29
2.5.3 Discussion.....	44

Chapter 3.....	46
Synthesis and characterization of Iron complex.....	46
3.1 Introduction	46
3.2 Synthesis and characterization of Fe (II)-thiol complex, Fe (II)- imidazole complex and Fe (II)-thiol-imidazole complex	46
3.2.1 Experimental plan	46
3.2.2 Experimental results	47
3.3 Synthesis and Characterization of Fe (II)-thiol-imidazole complex	48
3.3.1 Experimental plan	48
3.3.2 Experimental results	48
3.4 Synthesis of octanol soluble Fe (II) complex.	54
3.4.1 Experimental plan	54
3.4.2 Experimental results	54
3.4.3 Discussion.....	60
Chapter 4.....	61
POPC vesicles synthesis and metal complex in the membrane of vesicles.	61
4.1 Introduction	61
4.2. POPC vesicles synthesis and put metal complex in the membrane of vesicles.....	61
4.2.1 Experimental plan	61
4.2.2 Experimental results	61
4.3 Discussion	64
Chapter 5.....	65
Materials and Methods	65
5.1 Materials.....	65
5.2 Co (II) complex synthesis and Fe (II) complex synthesis	65
5.3 POPC Vesicles Synthesis.....	65
5.4 UV-Visible Absorption Spectroscopy	65
5.5 Saturation Binding Assay.....	66
5.6 Determination of K_d	66
5.7 ^{31}P NMR.....	66

Chapter 6.....	67
Conclusion and Future Work.....	67
References.....	69
Appendix.....	71

List of Tables

2.1. Picture of Co (II)-thiol-imidazole complex in the mixture of octanol and HEPES.	26
2.2. The UV-Vis spectra of Co (II) complex synthesized in the mixture of octanol and buffer.	45

List of Figures

1.1. Electronic absorption spectra of Cobalt (II) in tetracoordinate structural metal sites of proteins.....	6
2.1. The UV-Vis spectra of Co (II)- β -mercaptoethanol complex	8
2.2. The UV-Vis spectra of Co (II)- β -mercaptoethanol complex synthesized at various of pH values	9
2.3. The UV-Vis spectra of Co (II)- β -mercaptoethanol complex in different conditions.....	9
2.4. The UV-Vis spectra of Co (II)-DTT complex.....	10
2.5. The UV-Vis spectra of Co (II)-N-Acetyl-L-cysteine methyl ester complex.....	11
2.6. The UV-Vis spectra of Co (II)-imidazole complex.....	11
2.7. The UV-Vis spectra of Co (II) complex.....	13
2.8. The UV-Vis spectra of Co (II) complex.....	13
2.9. The UV-Vis spectra of Co (II)-N-Acetyl-L-cysteine methyl ester complex.....	14
2.10. The UV-Vis spectra of Co (II)- β -mercaptoethanol-imidazole complex.....	15
2.11. The UV-Vis spectra of Co (II)-N-Acetyl-L-cysteine methyl ester-imidazole complex.....	16
2.12. The UV-Vis spectra of Co (II) N-Acetyl-L-cysteine methyl ester-imidazole complex.....	16
2.13. The UV-Vis spectra of Co (II)-N-Acetyl-L-cysteine methyl ester-1-butylimidazole complex	17
2.14. The UV-Vis spectra of Co (II)-2-propanethiol-imidazole complex	18
2.15. The UV-Vis spectra of Co (II)-2-propanethiol-1-methylimidazole complex.....	18
2.16. The UV-Vis spectra of Co (II)-2-propanethiol-2-methylimidazole complex.....	19
2.17. The UV-Vis spectra of Co (II)-2-propanethiol-2-ethylimidazole complex.....	19

2.18. The UV-Vis spectra of Co (II)-2-propanethiol-1-butylimidazole complex.....	20
2.19. The UV-Vis spectra of Co (II)-benzenethiol-imidazole complex..	21
2.20. The UV-Vis spectra of Co (II)-benzenethiol-1-methylimidazole complex.....	21
2.21. The UV-Vis spectra of Co (II)-benzenethiol-2-methylimidazole complex.....	22
2.22. The UV-Vis spectra of Co (II)-benzenethiol-2-ethylimidazole complex.....	22
2.23. The UV-Vis spectra of Co (II)-benzenethiol-1-butylimidazole complex.....	23
2.24. The UV-Vis spectra of Co (II)-benzene-1,2-dithiol-imidazole complex.....	24
2.25. The UV-Vis spectra of Co (II)-benzene-1,2-dithiol-1-methylimidazole complex.....	24
2.26. The UV-Vis spectra of Co (II)-benzene-1,2-dithiol-1-butylimidazole complex	25
2.27. The UV-Vis spectra of Co (II)-benzene-1,2-dithiol-2-methylimidazole complex.....	25
2.28. The UV-Vis spectra of Co (II)-benzene-1,2-dithiol-2-ethylimidazole complex.....	26
2.29. The UV-Vis spectra of metal Cobalt titrations with N-Acetyl-L-cysteine methyl ester.....	30
2.30. Triplicate metal Cobalt titrations with N-Acetyl-L-cysteine methyl ester.....	31
2.31. The UV-Vis spectra of metal Cobalt titrations with 1-methylimidazole	32
2.32. Triplicate metal Cobalt titrations with 1-methylimidazole	33
2.33. Color for Co (II) complex.....	35
2.34. The UV-Vis spectra of Co (II)-N-Acetyl-L-cysteine methyl ester-1-butylimidazole complex	35
2.35. The UV-Vis spectra of Co (II)-N-Acetyl-L-cysteine methyl ester-1-butylimidazole complex	36
2.36. The UV-Vis spectra of Co (II)-N-Acetyl-L-cysteine methyl ester-1-butylimidazole complex	36

2.37. The UV-Vis spectra of Co (II)-N-Acetyl-L-cysteine methyl ester-1-butylimidazole complex	37
2.38. The UV-Vis spectra of Co (II)-N-Acetyl-L-cysteine methyl ester-butylimidazole complex in organic phase	37
2.39. The UV-Vis spectra of Co (II)-N-Acetyl-L-cysteine methyl ester-butylimidazole complex in aqueous phase	38
2.40. Color for Co (II) complex.....	39
2.41. The UV-Vis spectra of Co (II)-2-propanethiol-1-butylimidazole complex.....	39
2.42. The UV-Vis spectra of Co (II)-2-propanethiol-1-butylimidazole complex.....	40
2.43. The UV-Vis spectra of Co (II)-2-propanethiol-1-butylimidazole complex.....	40
2.44. The UV-Vis spectra of Co (II)-2-propanethiol-1-butylimidazole complex	41
2.45. The UV-Vis spectra of Co (II)-2-propanethiol-1-butylimidazole complex	41
2.46. The UV-Vis spectra of Co (II)-2-propanethiol-1-butylimidazole complex in organic phase	42
2.47. The UV-Vis spectra of Co (II)-2-propanethiol-1-butylimidazole complex in aqueous phase	42
2.48. The UV-Vis spectra of Co (II)-2-propanethiol-1-methylimidazole complex.....	44
2.49. The UV-Vis spectra of Co (II)-N-Acetyl-L-cysteine methyl ester-1-methylimidazole complex.....	44
3.1. The UV-Vis spectra of Iron titrations with N-Acetyl-L-cysteine methyl ester.....	47
3.2. The UV-Vis spectra of Iron titrations with 1-butylimidazole	48
3.3. The UV-Vis spectra of Fe (II)-N-Acetyl-L-cysteine methyl ester complex titrations with imidazole	49
3.4. The UV-Vis spectra of Fe (II)- N-Acetyl-L-cysteine methyl ester complex titrations with 1-methylimidazole.....	49
3.5. The UV-Vis spectra of Fe (II)-N-Acetyl-L-cysteine methyl ester complex titrations with 1-butylimidazole.....	50

3.6. The UV-Vis spectra of N-Acetyl-L-cysteine methyl ester titrations with Fe (II).....	50
3.7. The UV-Vis spectra of N-Acetyl-L-cysteine methyl ester and 1-butylimidazole titrations with Fe (II)	51
3.8. The UV-Vis spectra of N-Acetyl-L-cysteine methyl ester and 1-butylimidazole titrations with Fe (II)	51
3.9. The UV-Vis spectra of N-Acetyl-L-cysteine methyl ester and 1-butylimidazole titrations with Fe (II)	52
3.10. The UV-Vis spectra of N-Acetyl-L-cysteine methyl ester and 1-butylimidazole titrations with Fe (II)	52
3.11. The UV-Vis spectra of N-Acetyl-L-cysteine methyl ester and 1-butylimidazole titrations with Fe (II)	53
3.12. The UV-Vis spectra of N-Acetyl-L-cysteine methyl ester and 1-butylimidazole titrations with Fe (II)	53
3.13. Triplicate Iron titrations with N-Acetyl-L-cysteine methyl ester ..	55
3.14. The UV-Vis spectra of Fe (II)-N-Acetyl-L-cysteine methyl ester-1-butylimidazole complex	57
3.15. The UV-Vis spectra of Fe (II)-N-Acetyl-L-cysteine methyl ester-1-butylimidazole complex	57
3.16. The UV-Vis spectra of Fe (II)-N-Acetyl-L-cysteine methyl ester-1-butylimidazole complex	58
3.17. The UV-Vis spectra of Fe (II)-N-Acetyl-L-cysteine methyl ester-1-butylimidazole complex	58
3.18. The UV-Vis spectra of Fe (II)-N-Acetyl-L-cysteine methyl ester-1-butylimidazole complex	59
3.19. The UV-Vis spectra of Fe (II)-N-Acetyl-L-cysteine methyl ester-1-butylimidazole complex	59
3.20. The UV-Vis spectra of Fe (II) complex in organic phase	60
3.21. The color for Fe (II) complex.....	60
4.1. NMR spectra of POPC vesicles with different chemicals.....	62
4.2. NMR spectra of POPC vesicles with different chemicals.....	63
A.1. The UV-Vis spectra of Iron titrations with N-Acetyl-L-cysteine methyl ester.....	71
A.2. The UV-Vis spectra of Iron titrations with N-Acetyl-L-cysteine methyl ester.....	71

A.3. The UV-Vis spectra of Fe (II)- N-Acetyl-L-cysteine methyl ester complex titrations with 1-methylimidazole.....	72
A.4. The UV-Vis spectra of Fe (II)- N-Acetyl-L-cysteine methyl ester complex titrations with 1-butylimidazole.....	72

List of Abbreviations

Cys	Cysteine
DTT	Dithiothreitol
DNA	Deoxyribonucleic acid
HEPES	4-(2-hydroxyethyl)-1-piperazineethanesulfonic acid
HEPBS	N-(2-Hydroxyethyl)piperazine-N'-(4-butanesulfonic acid)
K _d	Dissociation constant
Min	Minute
nm	Nanometer
NMR	Nuclear magnetic resonance
POPC	1-palmitoyl-2-oleoyl-sn-glycero-3-phosphocholine
UV-Vis	Ultraviolet–Visible

Chapter 1

Introduction

1.1 The Origins of Life

'How life began' remains a long-lasting question that has intrigued people for centuries. Over thousands of years, people from different civilizations, thinkers and scientists from different eras gave their thoughts to this problem. In modern times, various possible scenarios have been explored by modern science to answer this question.

The idea that "Life was eternal and appeared spontaneously" was first started by Greek philosophy and Aristotle. Arising from this theory, "spontaneous generation" was generally accepted by Western scholarship until the 19th century.¹ Since the 17th century, experiments trying to explain "how life began" started to be published; however, several experimental results seemed to disprove the concept of spontaneous generation rather than prove it. For example, in 1864, after much evidence against the theory of spontaneous generation, Pasteur designed a simple experiment that largely ended belief in spontaneous generation. He used a series of flasks with long and twisted necks and then filled the flask with sterilized broth and urine. Pasteur showed that as long as the flask remained intact, nothing alive would emerge in the infusions. However, if the neck was broken, microbial growth was observed because of the introduction of microorganisms from the outside environment.² Pasteur's experiment seemed to indicate that life can only originate from pre-existing life.³

Darwin was the first scientist that combined chemistry with the 'origin of life'. In 1871, he proposed the idea to use the modern approach to study the chemical origin of life.¹ In 1953, a significant boost was given by Miller, he subjected a highly reduced mixture of gas including methane, ammonia, hydrogen, and water vapor to electric discharges and successfully obtained four amino acids--glycine, alanine, aspartic acid, and glutamic acid.⁴ Since then, a series of experiment showed that model prebiotic reactions in the laboratory can successfully synthesize the biomolecules that are the building blocks of life.

Nucleotides, amino acids, and lipids were synthesized prebiotically before life emerged.⁵ That is why most efforts focus on chemical reactions that either produce or exploit these molecules. However, in addition to their synthesis, the building blocks needed to be housed together to give rise to cell-like activity. This is typically achieved through encapsulation within lipid vesicles. Although there is debate as to whether encapsulation came early or late within a timeline between prebiotic chemistry and the Earth's first cells, most have come to think that the benefits of early encapsulation greatly outweigh the challenges.

Modern living systems use membranes to isolate from the extracellular aqueous environment. Additionally, the membrane can act as a boundary through which to achieve electron transfer between the internal volume and the external medium. Such membrane-based electron-transfer is useful for the storage and harnessing of energy and may represent an ancient process that helped keep protocells out of equilibrium. It is clear that extant life depends on metabolic-like chemistry that relies on the presence of membranes, but it is unclear when the dependence emerged. In other words, did the Earth's first cells also exploit electron transfer and proton gradients across membranes?

In modern cells, the membrane-based electron-transfer process could be achieved by exploiting a series of proteins with a complex, three-dimensional structure that inserts in the cell membrane. However, in the prebiotic world, proteins did not exist. Therefore, transition-metal redox pairs, which have a relatively simple structure may have provided the needed activity in the prebiotic world and may have achieved simple electron transfer across the membrane by donation and acceptance of electrons.

To put metal ions in the membrane, the charge carried by the metal ions and the hydrophobicity of the membrane-forming compound should be considered. The lipid molecule that could form the membrane of vesicles may have a hydrophobic tail and hydrophilic head. A metal ion carries a positive charge, so it may be difficult to put metal ions in the hydrophobic center of the membrane. A neutral metal complex in which the metal ion is coordinated by simple structure ligands could be easier to put in the hydrophobic center of the membrane. Such neutral complex could be synthesized by adjusting the charges carried by the ligands coordinated to the metal ions. For

example, a complex containing a divalent metal cation can be neutralized through the coordination of ligands that carry a net negative charge of two.

1.2 Lipid and membrane forming compound

The atmosphere of the prebiotic Earth was likely mostly nitrogen and carbon dioxide. No oxygen gas was present. Like the salty ocean today, the ocean of the early Earth would have contained dissolved salts, such as divalent alkaline earth cations in the millimolar range.⁶ At some point, compartmentalized boundaries emerged that contained the molecules needed for life.⁷ At the molecular level, the spontaneous appearance of closed membranes may be a prerequisite for the establishment of Darwinian evolution.⁵ Life as we know it needs boundaries, and compartmentalization gives many advantages to a nascent, life-like chemical system. Separation of the inner medium from the external medium makes it possible for the inner system to possess and maintain its own identity. The compartmentalized reactants could exist at a higher concentration, which could lead to higher rates of catalyses. The boundary can also achieve selective permeability and regularly exchange substances. Additionally, electron transfer based on the membrane could become an energy source to drive cellular activity.^{5,8}

All modern life is cellular.⁹ Contemporary cells are composed of amphiphilic molecules which have a nonpolar hydrocarbon tail and a polar headgroup. The molecules that can form the membrane of modern cells include phospholipids, cholesterol, and phospholipid ethers.¹⁰ Phospholipids are amphiphilic molecules that have a phosphorus head and two hydrocarbon tails that can be synthesized from fatty acids and glycerol. Phospholipids are amphiphilic molecules and can form modern compartment in which significant cellular activities happen, such as metabolism, transport of ions and the replication of molecules.¹¹

Complete phospholipids have been successfully synthesized under prebiotic conditions by Deamer, Oro and colleagues;¹²⁻¹⁶ however, different from the complex-structured lipids forming the modern cell membrane, on the early Earth, the membrane was likely formed by fatty acids, fatty alcohols, and phosphorylated derivatives.¹⁷ Under proper conditions, the mixture of these prebiotic amphiphilic molecules can self-

assemble into single layer micelles, double-layer vesicles in aqueous solution, and a monolayer at the interface of water and air. Such vesicles could encapsulate the organic species needed for a functioning cell, including a primitive genetic code, short peptides, and catalysts, and achieve energetic transduction.⁵ Bilayer vesicles are stabilized by the hydrophobic effect and van der Waals interactions and the formation of vesicles could also be affected by pH, temperature, the concentration of the salt, and the existence of some biopolymers.^{5,11,18,19} We can now synthesize vesicles under plausible prebiotic conditions in the lab to explore the scenarios of compartment formation on the primitive Earth.

1.3 Metal in the prebiotic world

Life is completely dependent on metal ions. The folding of RNA and protein is mostly performed by the coordination of metal ions, and metal centers play a significant role in the active sites of protein and RNA enzymes. An estimate showed that about half of all proteins carry a metal, and metal ions acting as cofactors are required in about one-third of known enzymes.^{20,21}

The First-Row transition metals Iron, Zinc, Cobalt, Manganese, and Copper represent the majority of the metal cofactors found in biology and play significant roles in cellular functions.²² In metalloproteins, metal ions are usually coordinated to the donor group nitrogen, oxygen, or sulfur centers from the amino acid sidechains of the protein. Sulfur, nitrogen, and oxygen centers are mostly provided by the thiolate group from cysteine,²³ imidazole group from histidine,²⁴ and carboxylate groups from aspartate and glutamate, respectively.²⁵ The deprotonated amides and carbonyl oxygen of the amide group from peptide backbones can also act as electron donors to the metal centers. Besides the amino acid residue from the protein, the ligands coordinated to metal ions can also be organic cofactors.²⁴

In the prebiotic world, proteins with complex structures could not have existed. Contemporary metalloproteins could have evolved from prebiotic metal catalysts. Metallocomplexes in which the metal ion is coordinated by organic ligands or short peptides may have existed on the early Earth and performed important roles in prebiotic catalysis.²⁶ Some of the transition metals of the fourth-period can remain stable in

multiple oxidation state, e.g., Fe (III) and Fe (II), Co (III) and Co (II), Cu (II) and Cu (I).²⁷ Therefore, within metal complexes, the metal center could be a redox pair achieving the acceptance and donation of electrons.

Among the transition metals, Iron is found in great quantities in animals and plays a significant role in biochemical systems. In modern cells, Iron can bind with proteins to form metalloproteins and act as cofactors to mediate catalytic processes. Iron proteins are also involved in the process of electron transfer. On the early Earth, these complex three-dimensional Iron proteins did not exist. Most Iron in the prebiotic world existed in a form of dissolved Iron (II) complexes. Therefore, with simple structure, Iron (II) complexes, in which Iron (II) was coordinated by small peptides or organic compounds could have played a similar role in electron transfer as Iron protein in the modern world. For example, Iron could have been coordinated to sulfur sites of cysteine residues of peptides to form Iron-sulfur peptides, and Iron-sulfur peptides were found to be a cofactor of electron transfer and may have existed in the prebiotic world.²⁸

1.4 Cobalt complex used as a spectroscopic probe.

Cobalt ions display characteristic spectra. The UV-Vis spectra of some Cobalt-substituted proteins and Cobalt-peptide complexes indicated that the Co (II)-thiolate complex with different number of thiolate ligands exhibited different spectra. In the series CoS_4 (Figure 1.1A), CoS_3N (Figure 1.1B), CoS_2N_2 (Figure 1.1C), and CoSN_3 (Figure 1.1D), as the number of the thiolate coordinated to Co (II) increases, the wavelengths of the absorption maxima steadily decrease. Thus, the UV-Vis spectra can be used as an efficient spectroscopic probe to distinguish the difference between the Co (II)-thiolate complex with different types of coordination.²⁹

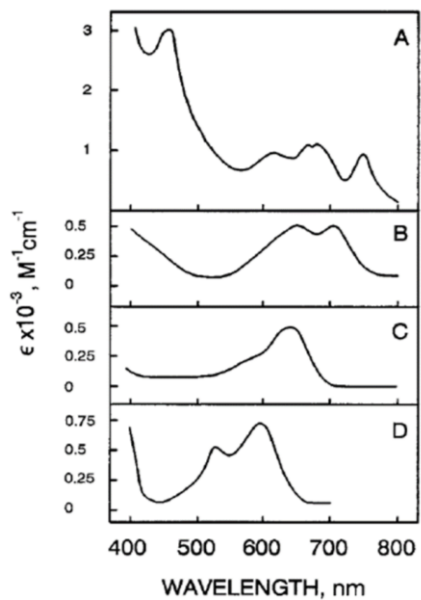


Figure 1.1. Electronic absorption spectra of Cobalt (II) in tetra-coordinate structural metal sites of proteins. (A) Coordination environment: COS_4 , Co (II)-substituted rubredoxin (B) Coordination environment: CoS_3N , Co (II) zinc box peptide, and (C) coordination environment: CoS_2N_2 , Co (II) zinc finger peptide (D) Coordination environment: CoSN_3 , complex of Co (II)-substituted insulin with pentafluorothiophenol. (Adapted from Maret, W and Vallee, B.L.)²⁹

Chapter 2

Synthesis and characterization of Cobalt complex.

2.1 Introduction

Prior studies showed that liposomes self-assembled from amphiphilic lipids could serve as possible models of protocellular systems in the prebiotic world.³⁰ To understand prebiotic compartmentalization, the bilayer lipid vesicles are synthesized in the lab to mimic the protocellular systems.³¹ Metalloprotein, acting as natural catalysts, play an important role in some of the most significant biological reactions in nature. Comparing to the complex, three-dimensional structures of extant metalloproteins, the prebiotic metallocomplexes could have a relatively simple structure. Such metallocomplexes could suggest as a biocatalyst to be evolved to the existing metalloproteins. My project is to adjust the charges carried by metallocomplexes by the number and type of ligands and try to put the metallocomplexes with no charge in the lipid membrane of the vesicles. The neutral metallocomplexes in the lipid membrane of vesicles could accept and donate electrons by the oxidation and reduction of metal ions, which may achieve the transfer of electrons across the lipid membrane.

The number of charges carried by metal complex can be adjusted by the number and type of ligands bound to the metal ion. Co (II) is a very useful spectroscopic probe of the ligand environment. The UV-Vis spectra of Cobalt complexes show clearly how many thiol-containing ligands are coordinated with Co (II), which helps to tell the structure of the complex and the charge carried by the complex. Co (II) coordinated with four thiols will have a band at around 750 nm. Co (II) coordinated with three thiols will have a band at around 700 nm. Co (II) coordinated with two thiols will have a band at around 650 nm. Co (II) coordinated with one thiol will have a band at around 600 nm.²⁹ In my project, the neutral Co (II)-thiol-imidazole complex that was aimed to be put in the membrane of vesicles was synthesized and the number of thiol ligands coordinated with Co (II) could be indicated by the UV-Vis spectra.

2.2 Synthesis and characterization of Co (II)-thiol and Co (II)-imidazole complex

2.2.1 Experimental plan

To find the best condition for the neutral Co (II)-imidazole-thiol complex formation, the Co (II) complex in which Co (II) was coordinated with only thiol-containing ligands or imidazole ligands were first synthesized in different conditions and evaluated by means of UV-Vis spectroscopy. The ligands we choose were imidazole and small thiol-containing molecules including β -mercaptoethanol, N-Acetyl-L-cysteine methyl ester, and DTT.

2.2.2 Co (II)- β -mercaptoethanol complex

The Co (II)- β -mercaptoethanol complex was synthesized in HEPES at different pH in an anaerobic environment. The UV-Vis spectra showed a band at around 750 nm which indicated that Co (II) was coordinated by four β -mercaptoethanol ligands. According to the UV-Vis spectra, pH = 8 was the best condition for Co (II)-thiol complex synthesis.

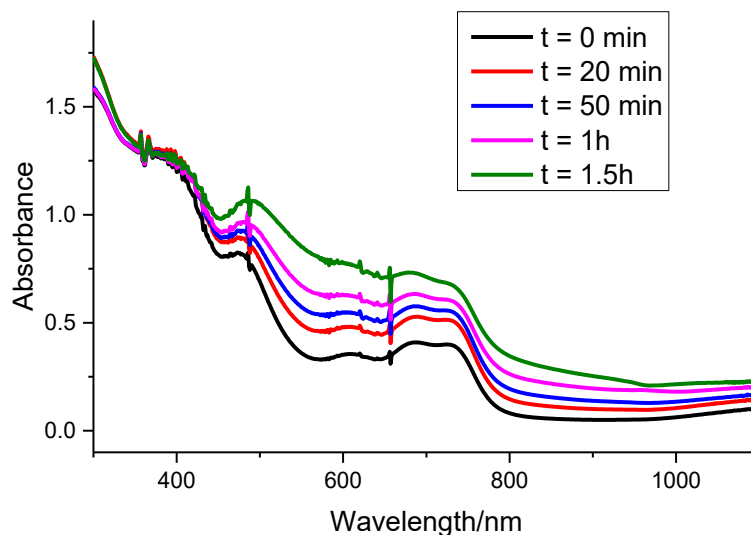


Figure 2.1. The UV-Vis spectra of Co (II)- β -mercaptoethanol complex, 1 mM Co (II), 28.5 mM β -mercaptoethanol and 100 mM HEPES, pH 8 was used.

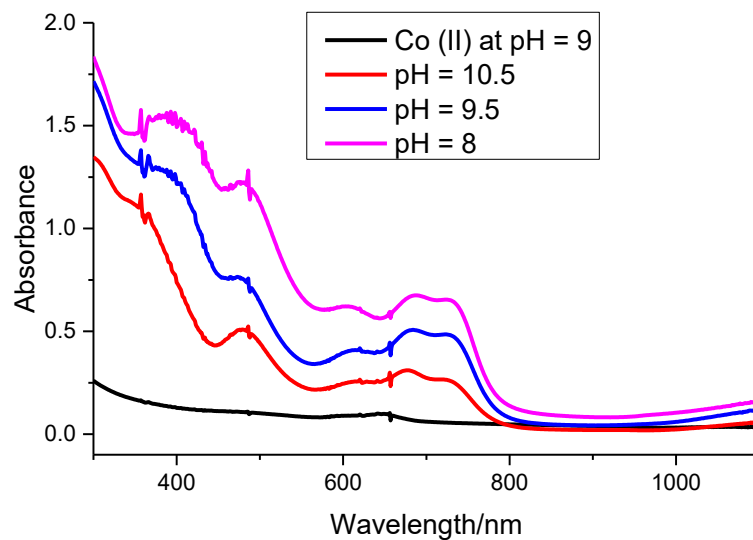


Figure 2.2. The UV-Vis spectra of Co (II)- β -mercaptoethanol complex synthesized at various of pH values, 1 mM Co (II), 28.5 mM β -mercaptoethanol, and 100 mM HEPES, was used.

When the Co (II)- β -mercaptoethanol complex was transferred from anaerobic environment to aerobic environment, a red precipitate appeared in the solution due to the oxidation of Co (II).

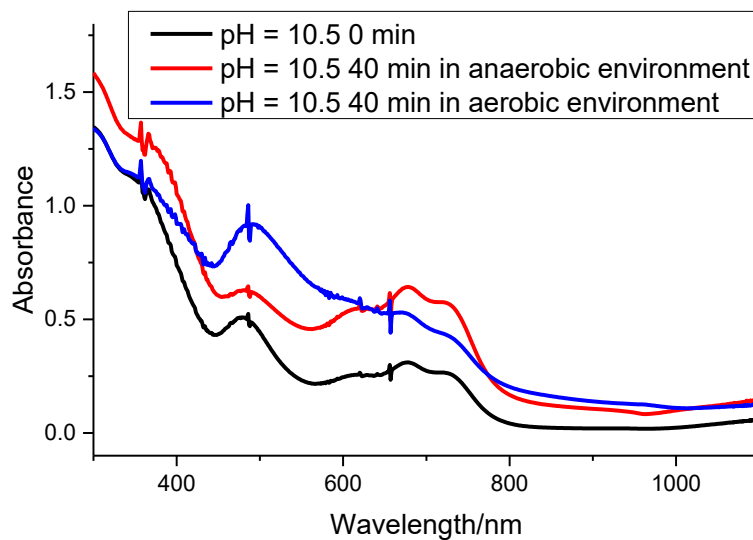


Figure 2.3. The UV-Vis spectra of Co (II)- β -mercaptoethanol complex in different conditions, 1 mM Co (II), 28.5 mM β -mercaptoethanol and 100 mM HEPES, pH 8 was used.

2.2.3 Co (II)-DTT complex

The Co (II)-DTT complex was synthesized in HEPES, pH 8 in anaerobic environment. The band at around 750 nm in the UV-Vis spectra indicated that Co (II) was coordinated with four thiolates.

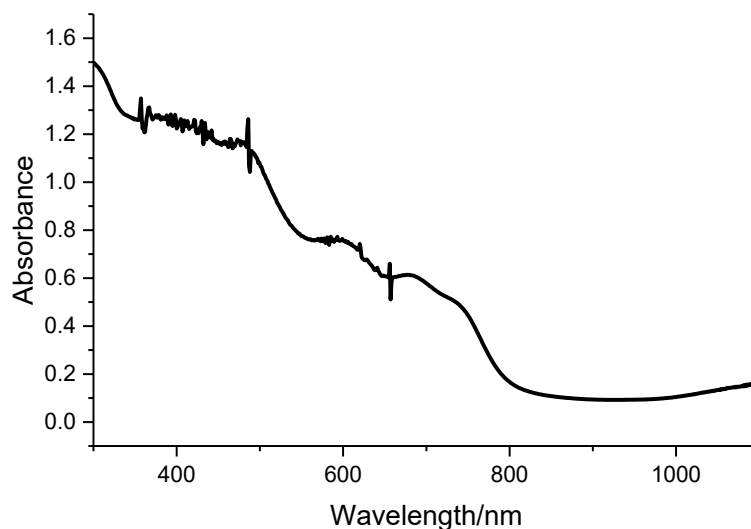


Figure 2.4. The UV-Vis spectra of Co (II)-DTT complex, 1 mM Co (II), 2.5 mM DTT, 100 mM HEPES, pH 8 was used.

2.2.4 Co (II)-N-Acetyl-L-cysteine methyl ester complex

Co (II)-N-Acetyl-L-cysteine methyl ester complex was synthesized in HEPES, pH 8 in anaerobic environment. The tetrahedral structure of Co (II) complex was indicated by the band at around 750 nm in the UV-Vis spectra.

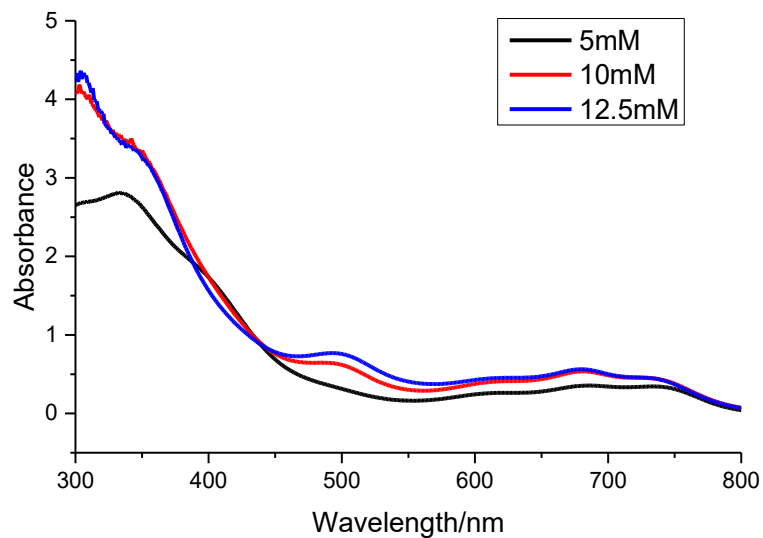


Figure 2.5. The UV-Vis spectra of Co (II)-N-Acetyl-L-cysteine methyl ester complex, 1 mM Co (II), N-Acetyl-L-cysteine methyl ester of various concentration and 100 mM HEPES, pH 8 was used.

2.2.5 Co (II)-imidazole complex

Co (II)-imidazole complex was synthesized in HEPES, pH 7 with different concentrations of Co (II) and imidazole in an anaerobic environment.

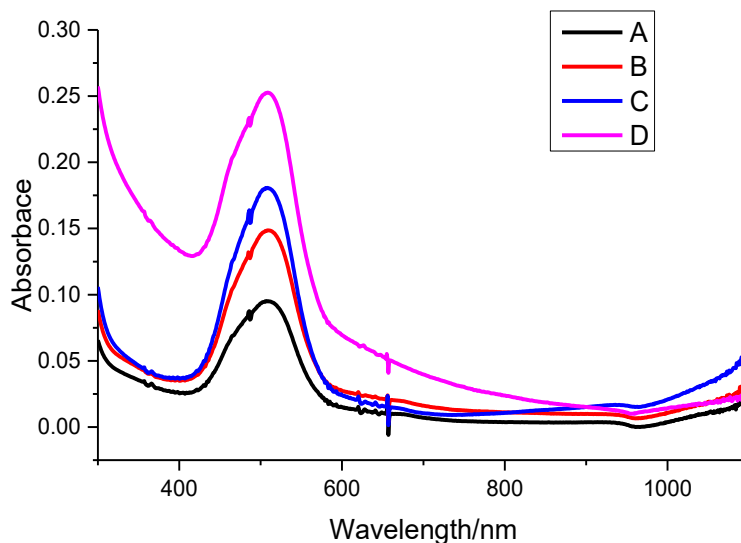


Figure 2.6. The UV-Vis spectra of Co (II)-imidazole complex, Co (II) and imidazole of various concentration, and 100 mM HEPES, pH 8 was used: A: 10 mM Co (II), 40 mM imidazole; B: 15 mM Co (II), 60 mM imidazole; C: 20 mM Co (II), 60 mM imidazole; D: 20 mM Co, 80 mM imidazole.

The band near 500 nm in the UV-Vis spectrum indicated that Co (II) was coordinated by four imidazole ligands.³²

2.3 Synthesize and characterization of Co (II)-thiol-imidazole complex

2.3.1 Experimental plan

At pH 8, the thiol-containing ligands carried one negative charge and imidazole was neutral. To synthesize a neutral Co (II) complex which could be inserted in the membrane of vesicles, the Cobalt complex coordinated with two thiol containing ligands and two imidazole ligands should be obtained.

The Cobalt complexes with thiol ligands and imidazole ligands were prepared in HEPES, pH 8 in an anaerobic environment. Different ratios of the two ligands were used, trying to find the suitable condition to synthesize the complex with two thiol ligands and two imidazole ligands. The number of the thiols that was coordinated to Co (II) could be indicated by UV-Vis spectra. N-Acetyl-L-cysteine methyl ester, β -mercaptoethanol and imidazole were chosen as ligands.

2.3.2 Co (II)- β -mercaptoethanol-imidazole complex and Co (II)-N-Acetyl-L-cysteine methyl ester-imidazole complex

The band at around 625 nm in UV-Vis spectra showed that Co (II)- β -mercaptoethanol-imidazole and Co (II)-N-Acetyl-L-cysteine methyl ester-imidazole complex with two thiol and two imidazole were successfully synthesized (CoS_2N_2). The structure of Cobalt complex indicated the neutral complex may be synthesized successfully.

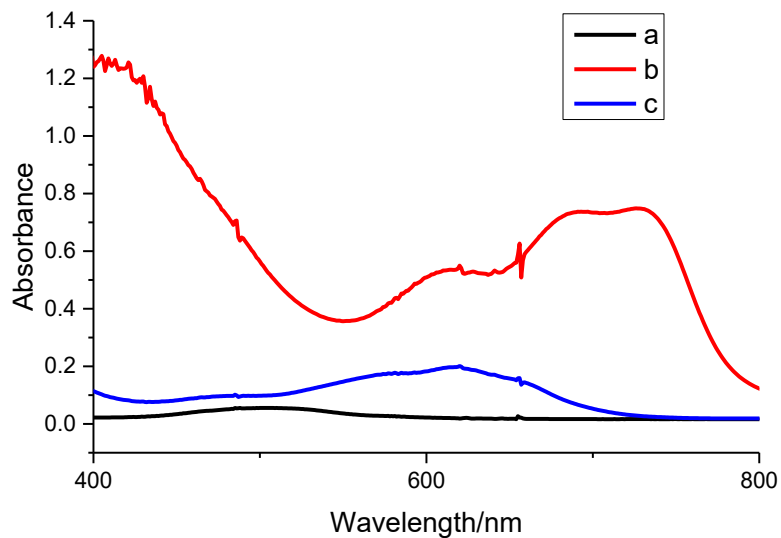


Figure 2.7. The UV-Vis spectra of Co (II) complex, 25 mM β -mercaptoethanol, 100 mM imidazole, 2 mM Co (II), and 100 mM HEPES, pH 8 was used: a: Co (II)-imidazole complex; b: Co (II)- β -mercaptoethanol complex; c: Co (II)- β -mercaptoethanol-imidazole complex.

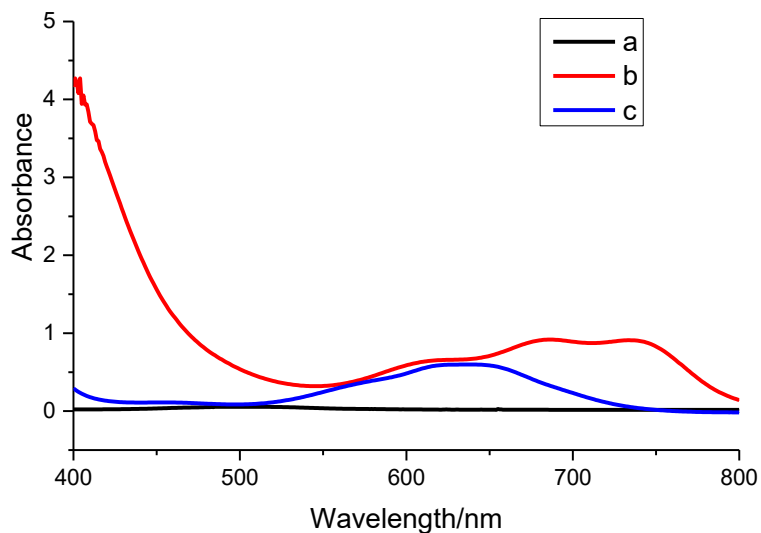


Figure 2.8. The UV-Vis spectra of Co (II) complex, 12.5 mM N-Acetyl-L-cysteine methyl ester, 100 mM imidazole, 2 mM Co (II), 100 mM HEPES, pH 8 was used: a: Co (II)-imidazole complex; b: Co (II)-N-Acetyl-L-cysteine methyl ester complex; c: Co (II)-N-Acetyl-L-cysteine methyl ester-imidazole complex.

The UV-Vis spectra indicated that Co (II)-thiol-imidazole complex was sensitive to oxygen. After transfer from an anaerobic environment to an aerobic environment, the absorbance of the peak at around 500 nm kept increasing, and a red

precipitate showed up in the solution of Co (II) complex, which meant the destroying of the tetrahedral structure of the Co (II) complex.

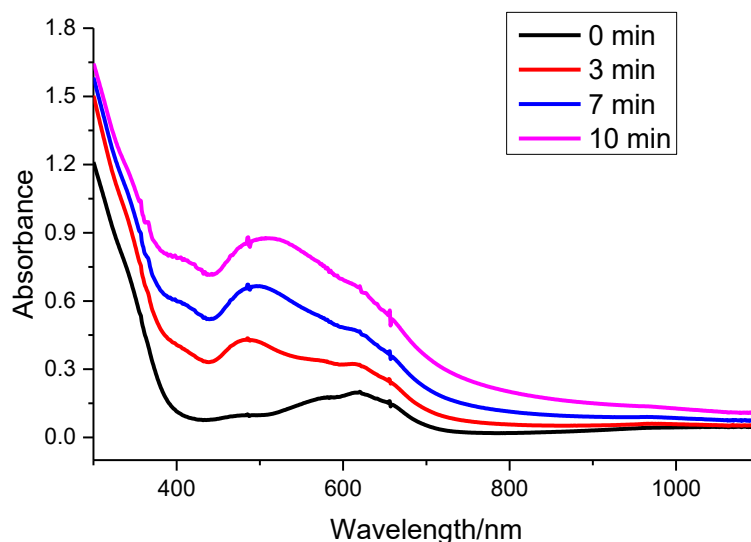


Figure 2.9. The UV-Vis spectra of Co (II)-N-Acetyl-L-cysteine methyl ester complex, 15 mM N-Acetyl-L-cysteine methyl ester, 100 mM imidazole, 2 mM Co (II), 100 mM HEPES, pH 8 was used.

2.4 Synthesis and characterization of Co (II)-imidazole-thiol complex in the mixture of octanol and HEPES

2.4.1 Experimental plan

On the early Earth, membranes were likely formed by fatty molecules such as fatty acids, alcohols with monoalkyl chain and double chain alkyl phosphates.¹⁷ The organic solvents decane, decanol and octanol were used to mimic the environment within a lipid membrane of vesicles. The Co (II) complex with both thiol-containing ligands and imidazole ligands were synthesized in a mixture of organic solvent and HEPES, pH 8 in an anaerobic environment and evaluated by means of UV-Vis spectroscopy. The UV-Vis spectra showed in which layer the Cobalt complex migrated to. The Co (II) complex that migrated to the organic phase could be put in the membrane of the vesicles. The ligands we choose were small thiol-containing molecules, including β -mercaptoethanol, N-Acetyl-L-cysteine methyl ester, 2-propanethiol, benzenethiol, and benzene-1,2-dithiol, imidazole, and its derivatives including 1-methylimidazole, 2-ethylimidazole, 2-methylimidazole and 1-butylimidazole.

2.4.2 Experimental Results

2.4.2.1 Co (II) complex with β -mercaptoethanol

The UV-Vis spectra showed that Co (II)- β -mercaptoethanol-imidazole complex with two thiol ligands and two imidazole ligands was soluble in buffer, not in organic solvent. Co (II)-N-Acetyl-L-cysteine methyl ester-imidazole complex with two thiols and two imidazole ligands complex was soluble in buffer and was insoluble in organic solvent.

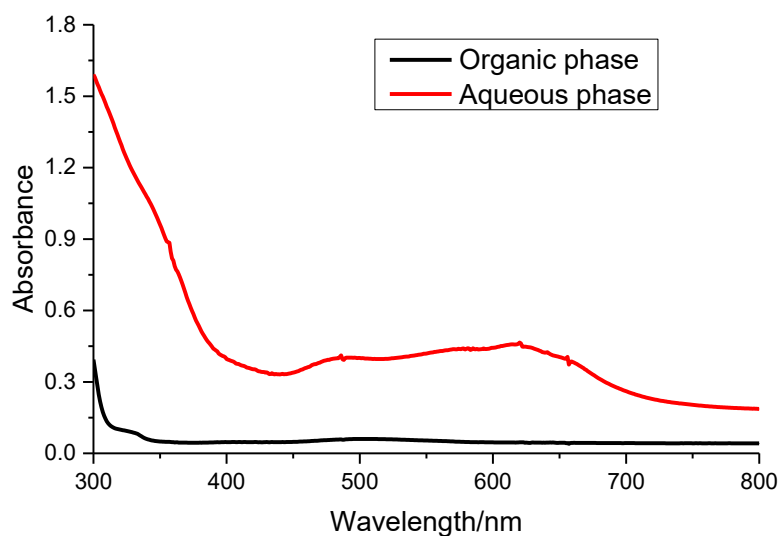


Figure 2.10. The UV-Vis spectra of Co (II)- β -mercaptoethanol-imidazole complex, 25 mM β -mercaptoethanol, 100 mM imidazole, 2 mM Co (II), the mixture of decane and 100 mM HEPES, pH 8 was used.

2.4.2.2 Co (II) complex with N-Acetyl-L-cysteine methyl ester

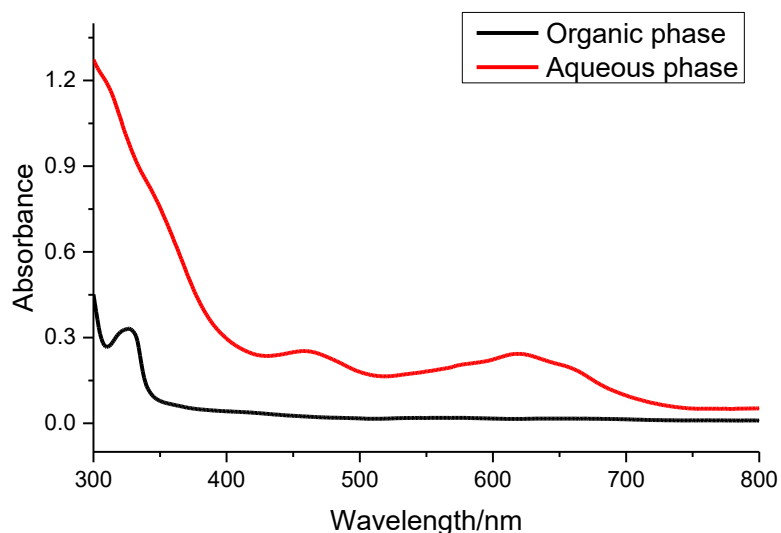


Figure 2.11. The UV-Vis spectra of Co (II)-N-Acetyl-L-cysteine methyl ester-imidazole complex, 12.5 mM N-Acetyl-L-cysteine methyl ester, 100 mM imidazole, 2 mM Co (II), the mixture of decane and 100 mM HEPES, pH 8 was used.

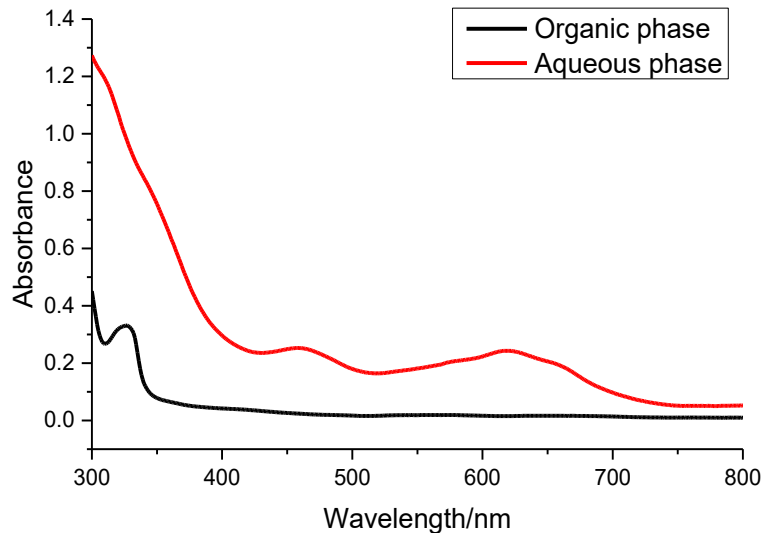


Figure 2.12. The UV-Vis spectra of Co (II) N-Acetyl-L-cysteine methyl ester-imidazole complex, 12.5 mM N-Acetyl-L-cysteine methyl ester, 100 mM imidazole, 2 mM Co (II), the mixture of decanol and 100 mM HEPES, pH 8 was used.

To increase the solubility of Co (II) complex in octanol, other imidazole derivatives with lower solubility in water such as 1-butylimidazole was used as ligands. After adding Co (II), N-Acetyl-L-cysteine methyl ester and 1-butylimidazole to the

mixture of octanol and buffer, Co (II) complex was firstly formed in buffer. After shaking the solvent mixture, complexes with two thiols and two 1-butylimidazole migrated into octanol. The mixture of Co (II) complex with different number of thiol ligands stayed in the buffer. The results showed that increasing the solubility of ligands in octanol could increase the solubility of Co (II) complex in octanol.

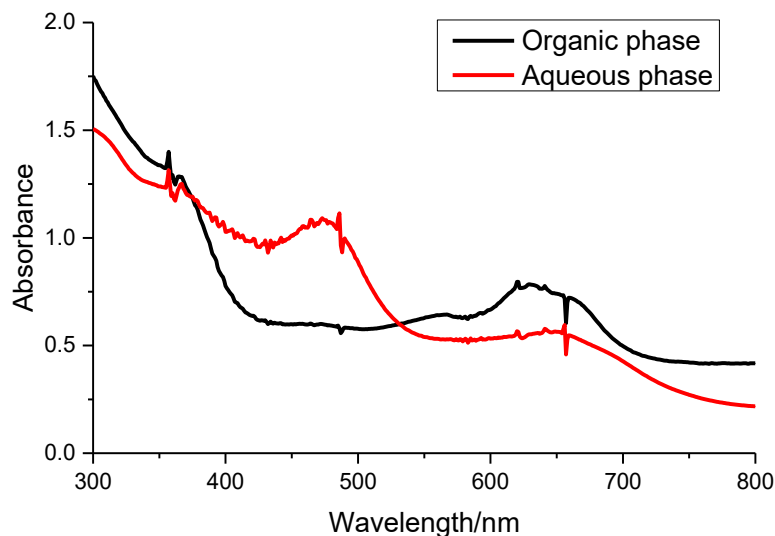


Figure 2.13. The UV-Vis spectra of Co (II)-N-Acetyl-L-cysteine methyl ester-1-butylimidazole complex, 10 mM N-Acetyl-L-cysteine methyl ester, 200 mM 1-butylimidazole, 2 mM Co (II), the mixture of octanol and 100 mM HEPES, pH 8 was used.

Five Co (II) complexes: Co (II)-2-propanethiol-imidazole complex, Co (II)-2-propanethiol-1-methylimidazole complex, Co (II)-2-methylimidazole complex, Co (II)-2-ethylimidazole-imidazole complex, Co (II)-1-butylimidazole complex were synthesized in the mixture of HEPES and octanol. After adding Co (II) and two different ligands to the solvent mixture and shaking, the complex was formed. The UV-Vis spectra indicated that, these five Co (II) complexes were all dissolved in octanol rather than in buffer, whereas their solubility in octanol was different due to the concentration of the ligands used and the solubility of the ligands in octanol and buffer (Figure 2.14-2.18). Using the imidazole ligands with a higher solubility in octanol and using a higher concentration of imidazole ligands to synthesize the complex could lead to a better result which was Co (II) complex obtained had a higher solubility in octanol. UV-Vis spectra of the organic phase showed a band near 625 nm that indicated the partitioning of a CoS_2N_2 complex in octanol.

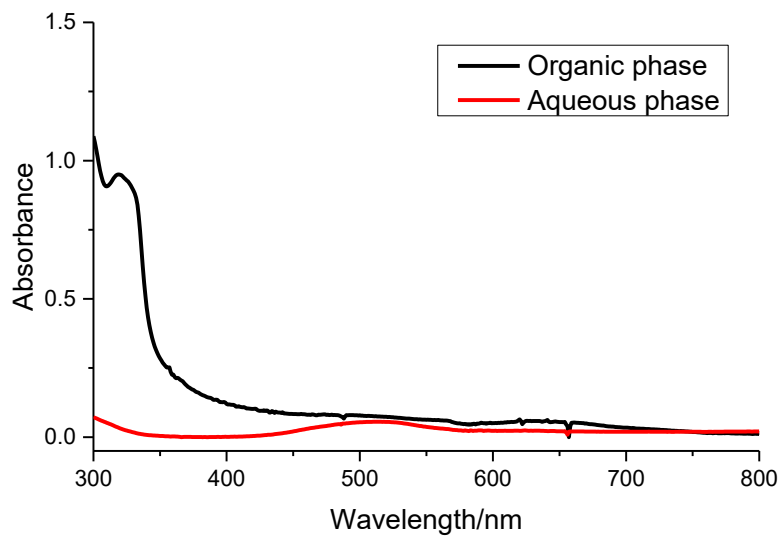


Figure 2.14. The UV-Vis spectra of Co (II)-2-propanethiol-imidazole complex, 215 mM 2-propanethiol, 200 mM imidazole, 2 mM Co (II), the mixture of octanol and 200 mM HEPES, pH 8 was used.

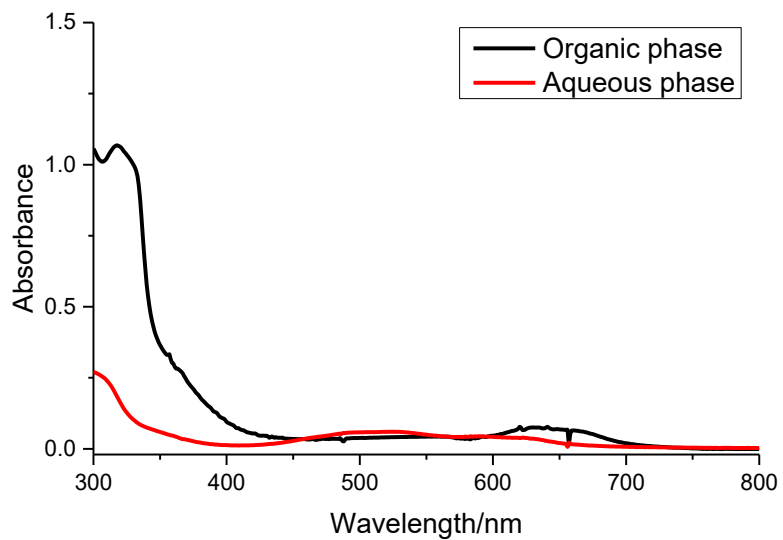


Figure 2.15. The UV-Vis spectra of Co (II)-2-propanethiol-1-methylimidazole complex, 161.5 mM 2-propanethiol, 200 mM 1-methylimidazole, 2 mM Co (II), the mixture of octanol and 200 mM HEPES, pH 8 was used.

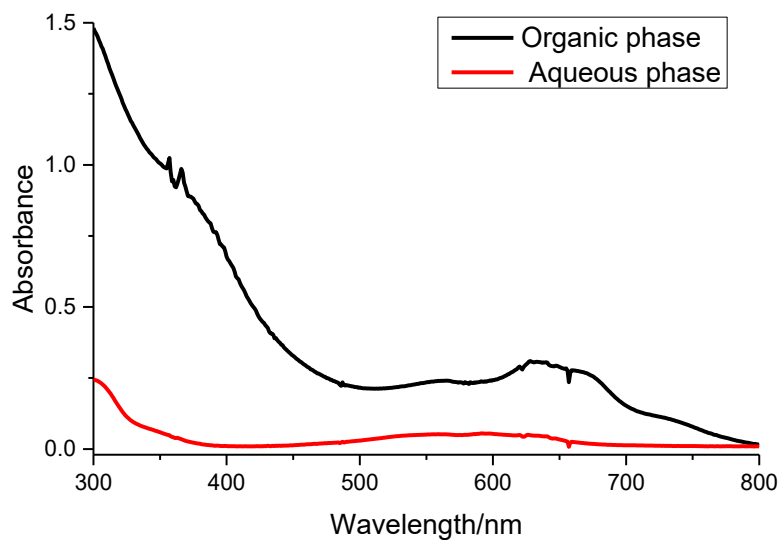


Figure 2.16. The UV-Vis spectra of Co (II)-2-propanethiol-2-methylimidazole complex, 161.5 mM 2-propanethiol, 100 mM 2-methylimidazole, 2 mM Co (II), the mixture of octanol and 200 mM HEPES, pH 8 was used.

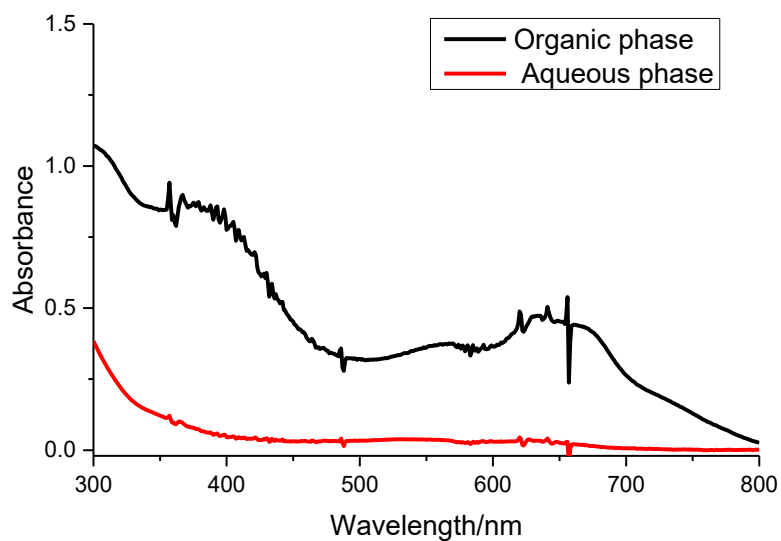


Figure 2.17. The UV-Vis spectra of Co (II)-2-propanethiol-2-ethylimidazole complex, 161.5 mM 2-propanethiol, 100 mM 2-ethylimidazole, 2 mM Co (II), the mixture of octanol and 200 mM HEPES, pH 8 was used.

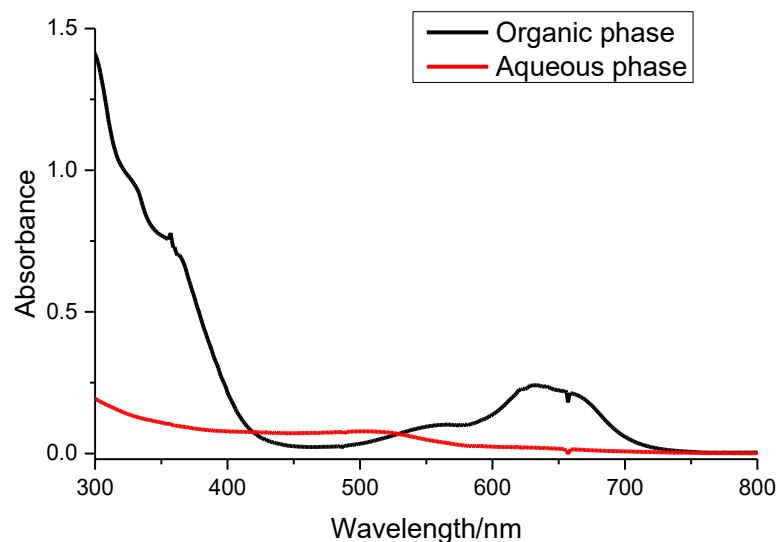


Figure 2.18. The UV-Vis spectra of Co (II)-2-propanethiol-1-butylimidazole complex, 161.5 mM 2-propanethiol, 200 mM 1-butylimidazole, 2 mM Co (II), the mixture of octanol and 200 mM HEPES, pH 8 was used.

Five Co (II) complex including Co (II)-benzenethiol-imidazole complex, Co (II)-Benzenethiol-1-methylimidazole complex, Co (II)-benzenethiol-2-methylimidazole complex, Co (II)-benzenethiol-2-ethylimidazole complex and Co (II)-benzenethiol-1-butylimidazole complex were synthesized in the mixture of HEPES and octanol. The Co (II) complex could be formed in octanol after adding Co (II) and ligands to the solvent mixture and shake. The UV-Vis spectra showed that, these five complexes all had a high solubility in octanol (Figure 2.19-2.23). This was probably due to the fact that benzenethiol was insoluble in water and soluble in octanol. The hydrophobicity of benzenethiol decreased the solubility of the Co (II) complex in water and made the complex insoluble in buffer. UV-Vis spectra of the organic phase showed a band around 630 nm, indicating that most of the Co (II) complex was soluble in octanol as a CoS_2N_2 complex, whereas the band at around 410 nm and 660 nm indicated the presence of a small amount of a CoS_3N complex in octanol.

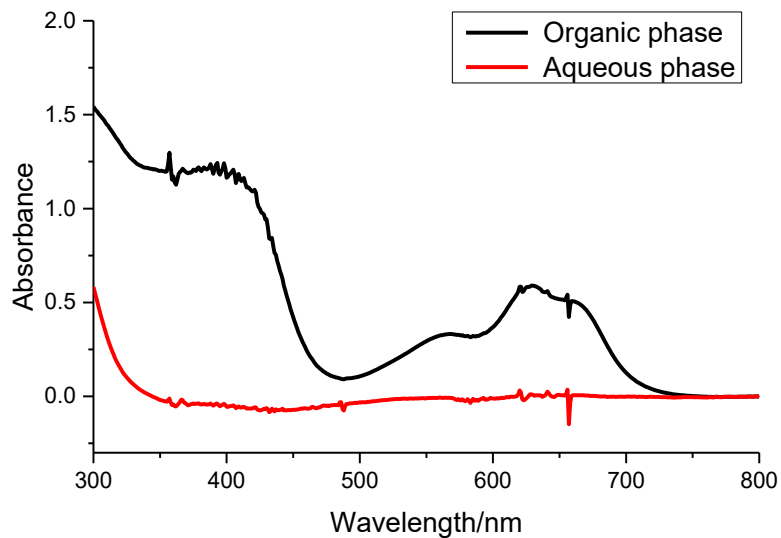


Figure 2.19. The UV-Vis spectra of Co (II)-benzenethiol-imidazole complex, 20 mM thiophenol, 100 mM imidazole, 2 mM Co (II), the mixture of octanol and 200 mM HEPES, pH 8 was used.

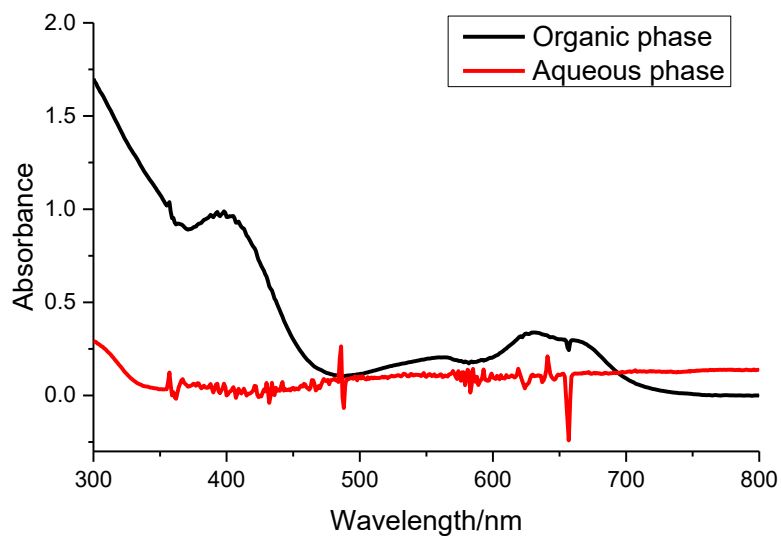


Figure 2.20. The UV-Vis spectra of Co (II)-benzenethiol-1-methylimidazole complex, 20 mM thiophenol, 50 mM 1-methylimidazole, 20 mM Co (II), the mixture of octanol and 200 mM HEPES, pH 8 was used. The points (620, 0.283955097), (621, 0.223610878), (622, 0.040977955), (623, 0.024381638), (655, 0.189370632), (656, 0.506653786) of aqueous spectrum were deleted to smooth the spectrum.

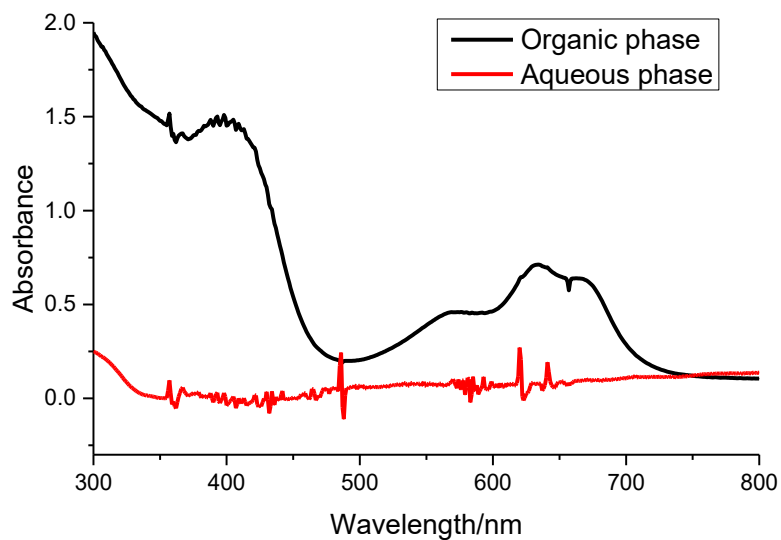


Figure 2.21. The UV-Vis spectra of Co (II)-benzenethiol-2-methylimidazole complex, 20 mM thiophenol, 100 mM 2-methylimidazole, 2 mM Co (II), the mixture of octanol and 200 mM HEPES, pH 8 was used. The points (655, 0.18044), (656, 0.55973), (657, -0.27058), (658, -0.06404) of aqueous spectrum were deleted to smooth the spectrum.

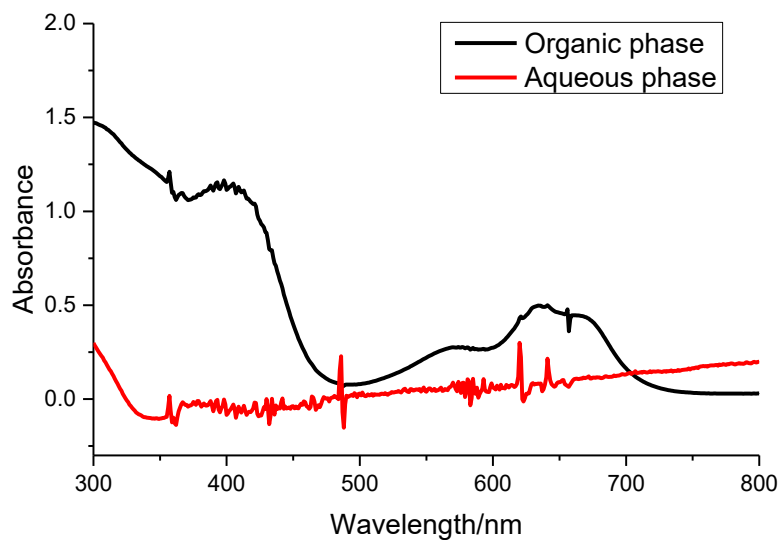


Figure 2.22. The UV-Vis spectra of Co (II)-benzenethiol-2-ethylimidazole complex, 20 mM thiophenol, 100 mM 2-ethylimidazole, 2 mM Co (II), the mixture of octanol and 200 mM HEPES, pH 8 was used. The points (655, 0.213026524), (656, 0.596318722), (657, -0.252451897), (658, -0.062920093) of aqueous spectrum were deleted to smooth the spectrum.

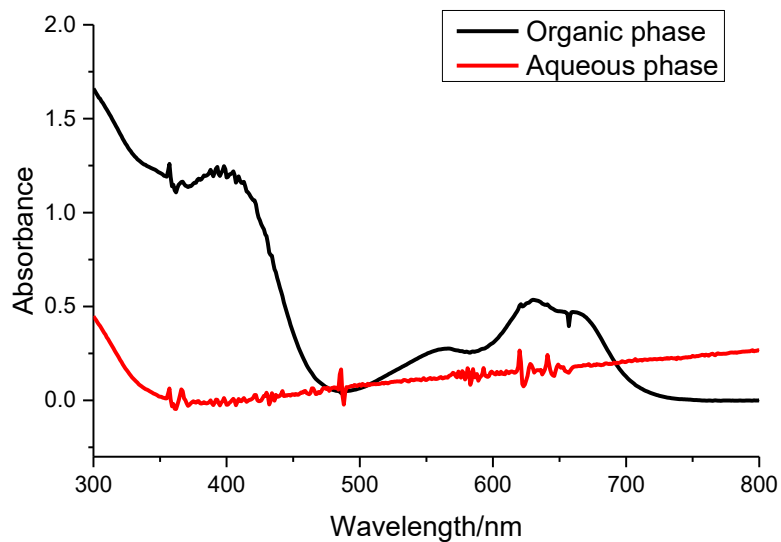


Figure 2.23. The UV-Vis spectra of Co (II)-benzenethiol-1-butylimidazole complex, 20 mM thiophenol, 100 mM 1-butylimidazole, 2 mM Co (II), the mixture of octanol and 200 mM HEPES, pH 8 was used. The points (655, 0.286696911) (656, 0.566367149) (657, -0.134506226) (658, 0.059768677) of aqueous spectrum were deleted to smooth the spectrum.

Five Co (II) complex were synthesized in the mixture of octanol and HEPES including Co (II)-benzene-1,2-dithiol-imidazole complex, Co (II)-benzene-1,2-dithiol-1-methylimidazole complex, Co (II)-benzene-1,2-dithiol-2-methylimidazole complex, Co (II)-benzene-1,2-dithiol-2-ethylimidazole complex, Co (II)-benzene-1,2-dithiol-1-butylimidazole complex. These five complexes were synthesized in octanol and the UV-Vis spectra showed that within the complex, Co (II) was coordinated with two thiol ligands and two imidazole ligands (Figure 2.24-2.28). The binding affinity of benzene-1,2-dithiol to Co (II) was very large, so the concentration of Co (II) and ligands being used was low, and the complex synthesized was very stable in octanol.

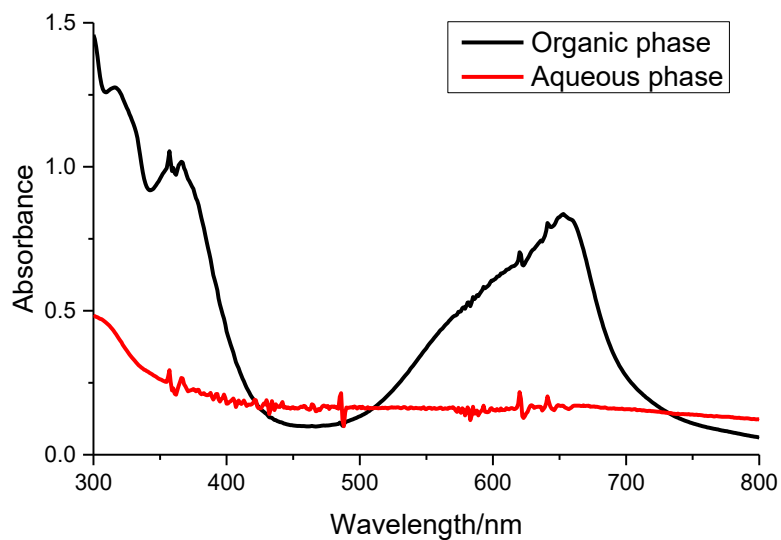


Figure 2.24. The UV-Vis spectra of Co (II)-benzene-1,2-dithiol-imidazole complex, 1.73 mM Benzene-1,2-dithiol, 10 mM imidazole, 0.4 mM Co (II), the mixture of octanol and 100 mM HEPES, pH 8 was used. The points (655, 0.19449) (656, 0.28194) (657, -0.05143) (658, 0.10435) of aqueous spectrum and (655, 0.86325) (656, 0.9518) (657, 0.64272) (658, 0.7691) of organic spectrum were deleted to smooth the spectrum.

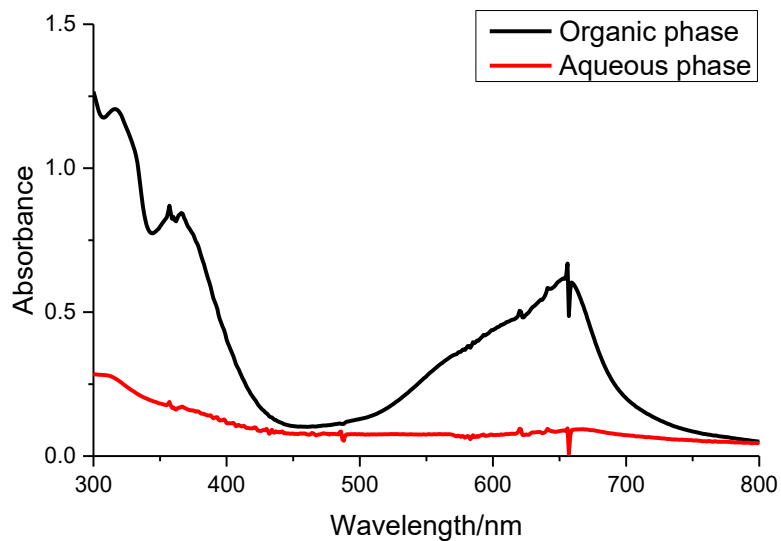


Figure 2.25. The UV-Vis spectra of Co (II)-benzene-1,2-dithiol-1-methylimidazole complex, 0.43 mM Benzene-1,2-dithiol, 25 mM 1-methylimidazole, 0.4 mM Co (II), the mixture of octanol and 100 mM HEPES, pH 8 was used.

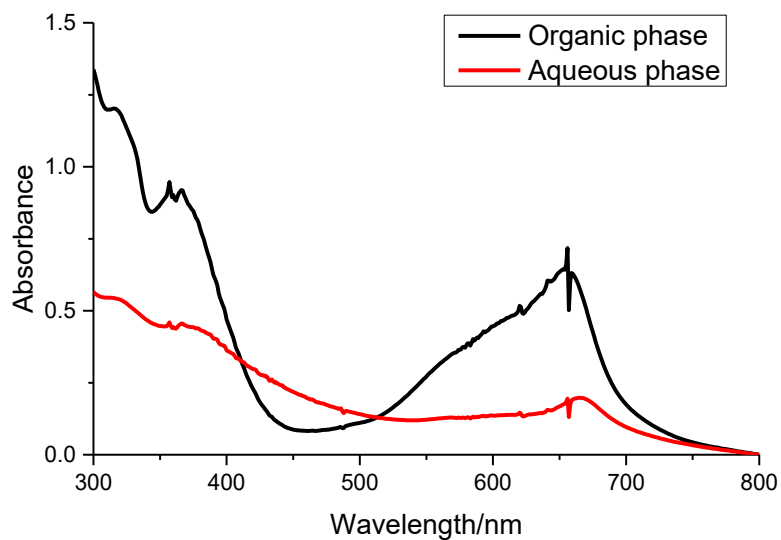


Figure 2.26. The UV-Vis spectra of Co (II)-benzene-1,2-dithiol-1-butylimidazole complex, 0.43 mM Benzene-1,2-dithiol, 5 mM 1-butylimidazole, 0.4 M Co (II), the mixture of octanol and 100 mM HEPES, pH 8 was used.

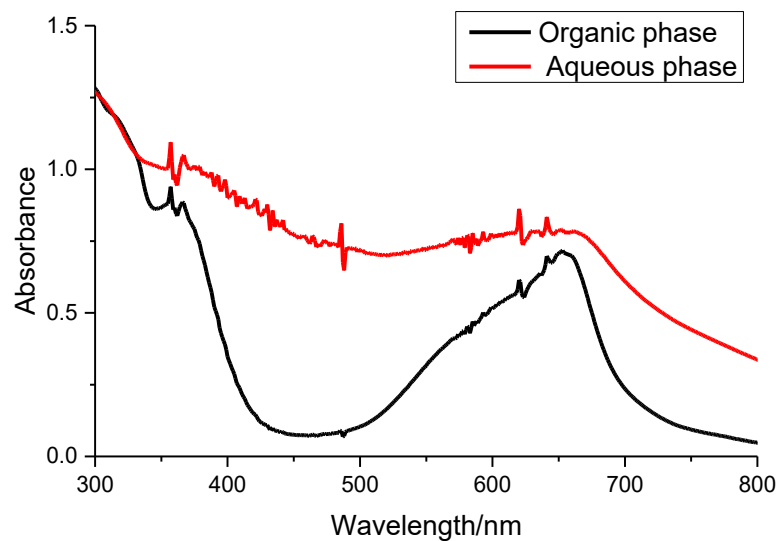


Figure 2.27. The UV-Vis spectra of Co (II)-benzene-1,2-dithiol-2-methylimidazole complex, 0.43 mM Benzene-1,2-dithiol, 10 mM 2-methylimidazole, 0.4 mM Co (II), the mixture of octanol and 100 mM HEPES, pH 8 was used. The points (655, 0.491117001) (656, 0.63824129) (657, 0.20867157) (658, 0.368612289) of aqueous spectrum and (655, 0.757179215) (656, 0.841350033) (657, 0.498666241) (658, 0.647233917) of organic spectrum were deleted to smooth the spectrum.

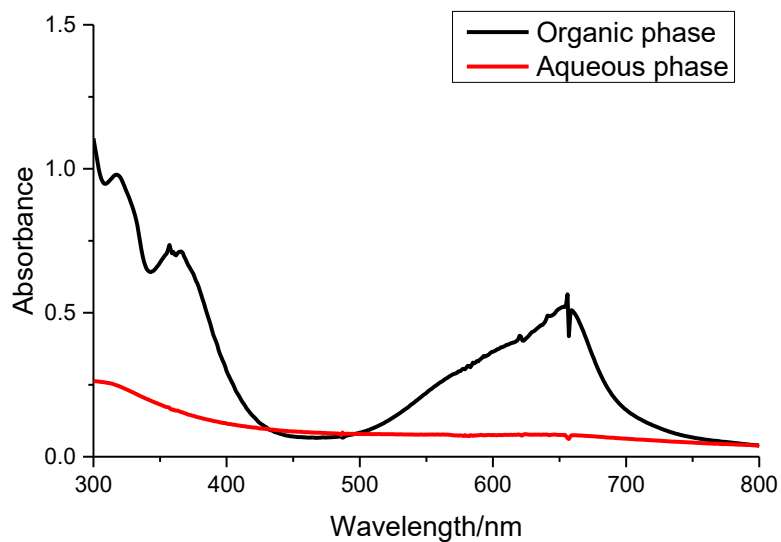


Figure 2.28. The UV-Vis spectra of Co (II)-benzene-1,2-dithiol-2-ethylimidazole complex, 0.43 mM Benzene-1,2-dithiol, 5 mM 2-ethylimidazole, 0.4 mM Co (II), the mixture of octanol and 100 mM HEPES, pH 8 was used.

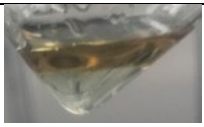
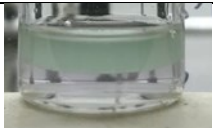
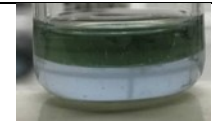
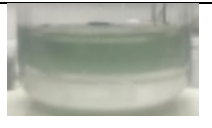
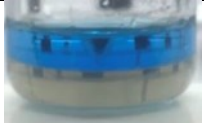
Cobalt complex synthesized in the mixture of octanol and buffer	imidazole Log P=-0.08	1-methylimidazole Log P=-0.06	2-methylimidazole Log P=0.24	2-ethylimidazole XLogP3-AA=0.9	1-butylimidazole XLogP3-AA=1.2
β -mercaptoethanol XLogP3-AA=-0.2	N/A			N/A	
N-Acetyl-L-cysteine methyl ester XLogP3=0.7					
2-propanethiol XLogP3-AA=1.3	N/A				
benzene-1,2-dithiol XLogP3=2.2					
benzenethiol XLogP3-AA=2.5					

Table 2.1. Picture of Co (II)-thiol-imidazole complex in the mixture of octanol and HEPES.³³

2.4.3 Discussion

The result of octanol soluble Co (II) complex synthesis indicated that, the solubility of Co (II) complex could be related to the solubility of ligands and concentration of ligands used to synthesize the complex. The concentration used is determined by the binding affinity of ligands to Co (II). Benzenethiol and benzene-1, 2-dithiol are insoluble in octanol, therefore, Co (II) complex in which Co (II) is coordinated with both benzenethiol and either of the five imidazole ligands are synthesized at the interface of octanol and buffer and then migrate to octanol. Co (II) complex with benzene-1,2-dithiol and either of the five imidazole ligands gave the same result. N-Acetyl-L-cysteine methyl ester has a high solubility in buffer, so the solubility of the imidazole ligands plays a significant role in solubility of Co (II) complex in octanol. Imidazole, 1-methylimidazole, 2-methylimidazole and 2-ethylimidazole have a higher solubility in water comparing to the water insoluble 1-butylimidazole. Therefore, Co (II) complex in which Co (II) is coordinated with N-Acetyl-L-cysteine methyl ester and either of these four imidazole ligands could be synthesized and preferred to stay in buffer and not migrate to octanol. Co (II) complex with N-Acetyl-L-cysteine methyl ester and 1-butylimidazole has a higher solubility in octanol, therefore, after synthesized in solvent mixture and shake, it could migrate to octanol from buffer. 2-propanethiol is soluble in water but it has a lower solubility in water than N-Acetyl-L-cysteine methyl ester. The Co (II) complex with 2-propanethiol and each of the five ligands used could all migrate to octanol, but different concentrations of different imidazole ligands were used. It may be because the solubility of Co (II) complex could be affected by the charges carried by the complex. The charges carried by Cobalt complex could be adjusted by the number of thiol ligands and imidazole ligands coordinated to Co (II). The number could be affected by the ratio of concentration of thiol ligands to imidazole ligands used, and such ratio of concentration used was determined by the binding affinity of ligands to Co (II). Therefore, binding affinity of ligands could be a factor that affects the formation of the structure of Co (II) complex, further, could be another factor to affect the solubility of Co (II)-thiol-imidazole complex in octanol.

In the UV-Vis spectra of CoS₂N₂ complex, the band at around 630 nm means that the solution of CoS₂N₂ complex absorbs orange wavelength, so the solution appears blue. For the UV-Vis spectra of the mixture of CoS₂N₂ complex and Co (II) complex of other forms, besides the band at around 630 nm, there is also a large peak at around 410 nm absorbing the purple wavelength, which makes the solution appears a mixed color of blue and yellow, so the solution of Co (II) complex appears bluish green. Table 1 shows the color of the organic phase and aqueous phase when synthesizing Co (II) complex in the mixture of octanol and buffer. The upper layer is the organic phase, and the lower layer is aqueous phase. When the Co (II) complex dissolves in octanol, the upper layer becomes bluish which indicated that it was CoS₂N₂ dissolved in octanol. Some Co (II) complex such as Co (II)-benzenethiol-imidazole complex is bluish green, indicating that in addition to CoS₂N₂, there may be a small amount of blue-green coloured CoS₃N dissolved in octanol. When the Co (II) complex dissolved in buffer, the lower layer becomes bluish, which indicated the presence of a CoS₂N₂ complex. CoS₂N₂ is sensitive to oxygen, and so the appearance of a bluish green color over time may indicate oxidation.

In table 2.1, the Log P of the ligands are listed. Log P (o/w) is an empirically determined parameter that indicates the partitioning of a chemical between octanol and water. For the ligands that have a Log P larger than 0, there is a preference to reside in the octanol phase.³⁴ XLogP3-AA is derived from the summation of the Log P values of each atom in a given molecule.³⁵ XLogP3 is a calculated value based on the known Log P of reference compounds.³⁵

2.5 Binding affinity of thiol-containing ligands and imidazole ligands to Co (II)

2.5.1 Experimental plan

To better understand how binding affinity of ligands-Co (II) coordination affected the solubility of Co (II) complex in octanol, based on the ligands' prebiotic properties and solubility in water, imidazole ligands including 1-methylimidazole and 1-butyylimidazole, thiol ligands including N-Acetyl-L-cysteine methyl ester and 2-

propanethiol were chosen to do a further study. K_d for Co (II)-thiol complex and Co (II)-imidazole complex were first calculated through competition experiment. Then Co (II) complex was synthesized using the thiol ligands and imidazole ligands with the concentration of value of K_d . The UV-Vis spectra could show in which layer the Cobalt complex partitioned to and could further demonstrate the relationship between the solubility of Co (II) complex in octanol and binding affinity of ligands-Co (II) coordination.

2.5.2 Experimental results

2.5.2.1 Binding affinity of N-Acetyl-L-cysteine methyl ester to Co (II)

For N-Acetyl-L-cysteine methyl ester, the final value of K_d was calculated as the average of the three values obtained in each single set of experiments. Figure 2.30 showed the results of the three replicates of N-Acetyl-L-cysteine methyl ester titrations of 5 mM Cobalt (II). For each of the three experiments, the trend of absorbance monitored at 750 nm (CoS_4) against the concentration of N-Acetyl-L-cysteine methyl ester was reported. The absorbance at 750 nm kept increasing until at around 14 mM N-Acetyl-L-cysteine was added to Co (II), after which little change in intensity of peak was observed (Figure 2.29, 2.30). These values were then fit to the Hill equation to determine the K_d of each of the three cases. The final K_d for N-Acetyl-L-cysteine methyl ester- Co (II) was 4.7 ± 0.2 mM (A. $K_d=4.915$ mM, $h=2.082$; B. $K_d=4.493$ mM, $h=1.878$; C. $K_d=4.603$ mM, $h=1.859$).

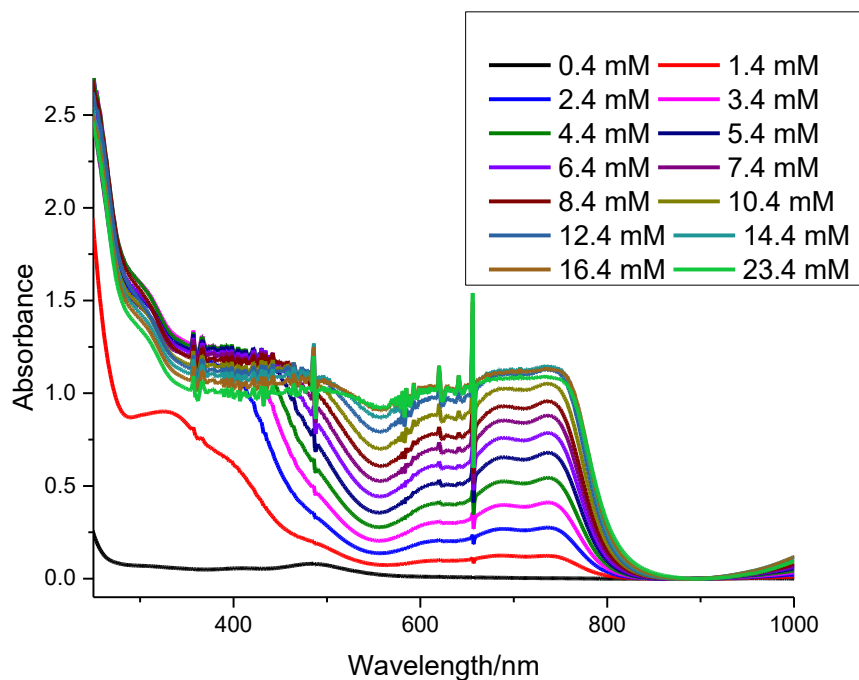
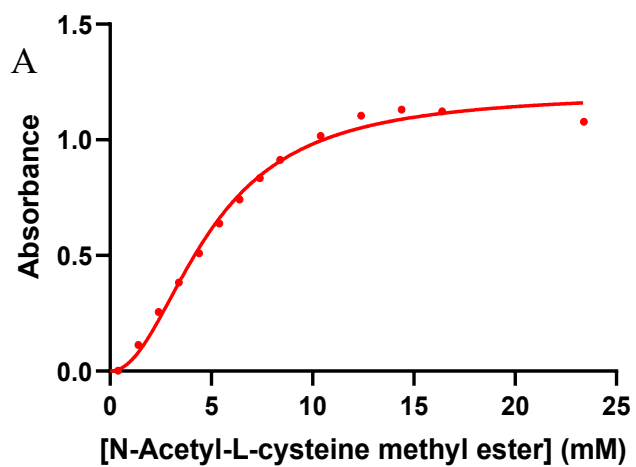


Figure 2.29. The UV-Vis spectra of metal Cobalt titrations with N-Acetyl-L-cysteine methyl ester. 5mM Co (II) and 100 mM HEPES, pH 8 was used.



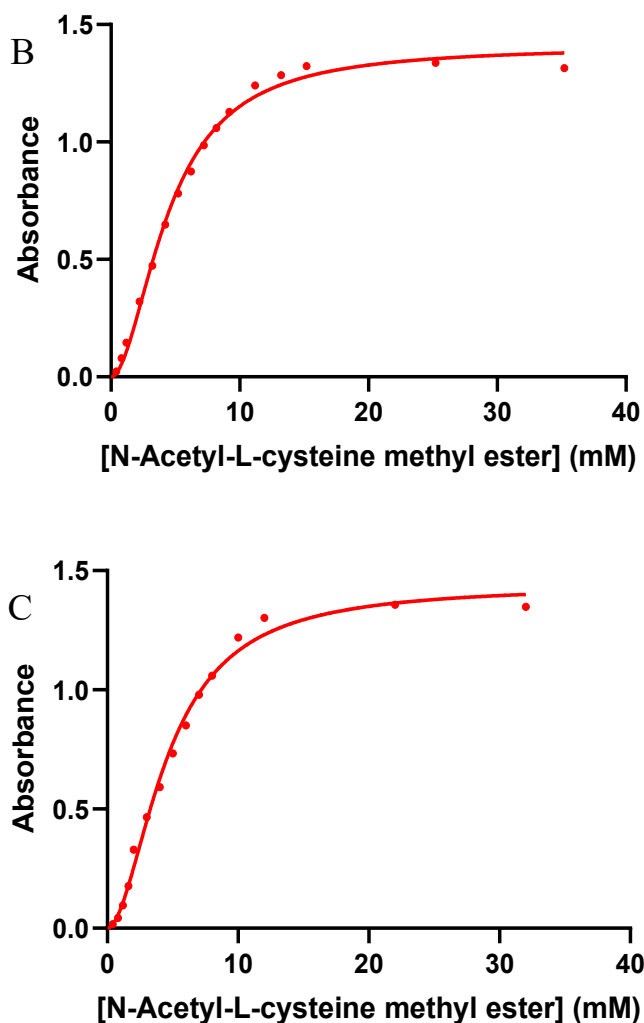


Figure 2.30. Triplicate metal Cobalt titrations with N-Acetyl-L-cysteine methyl ester. (A+B+C): N-Acetyl-L-cysteine methyl ester complex - dependent absorbance changed at 750 nm were monitored in the presence of 5 mM Co (II). The data was fit to the specific binding and Hill slope equation.

2.5.2.2 Binding affinity of 1-methylimidazole to Co (II)

For 1-methylimidazole, the final value of K_d was calculated as the average of the three values obtained in each single set of experiments. The results of the three replicates of 1-methylimidazole titrations of 5 mM Cobalt (II) were shown in Figure 2.32. The trend of absorbance monitored at 500 nm (CoN_4) against the concentration of 1-methylimidazole was reported for each of the three experiments. Figure 2.31 and 32 showed that absorbance at 500 nm kept increased until at around 50 mM 1-methylimidazole was added to Co (II), after which little change in intensity of peak was

observed. These values were then fit to the Hill equation to determine the K_d for each of these three cases. The final K_d for 1-methylimidazole-Co (II) coordination was 30 ± 10 mM (A. $K_d=38.83$ mM, $h=0.3789$; B. $K_d=17.18$ mM, $h=0.4182$; C. $K_d=33.10$ mM, $h=0.4118$).

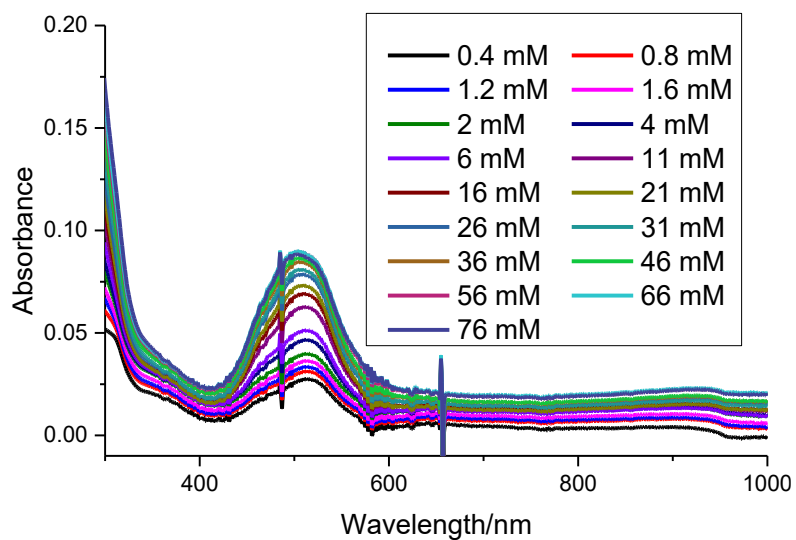


Figure 2.31. The UV-Vis spectra of metal Cobalt titrations with 1-methylimidazole. 5 mM Co (II), 100 mM HEPES, pH 8 was used

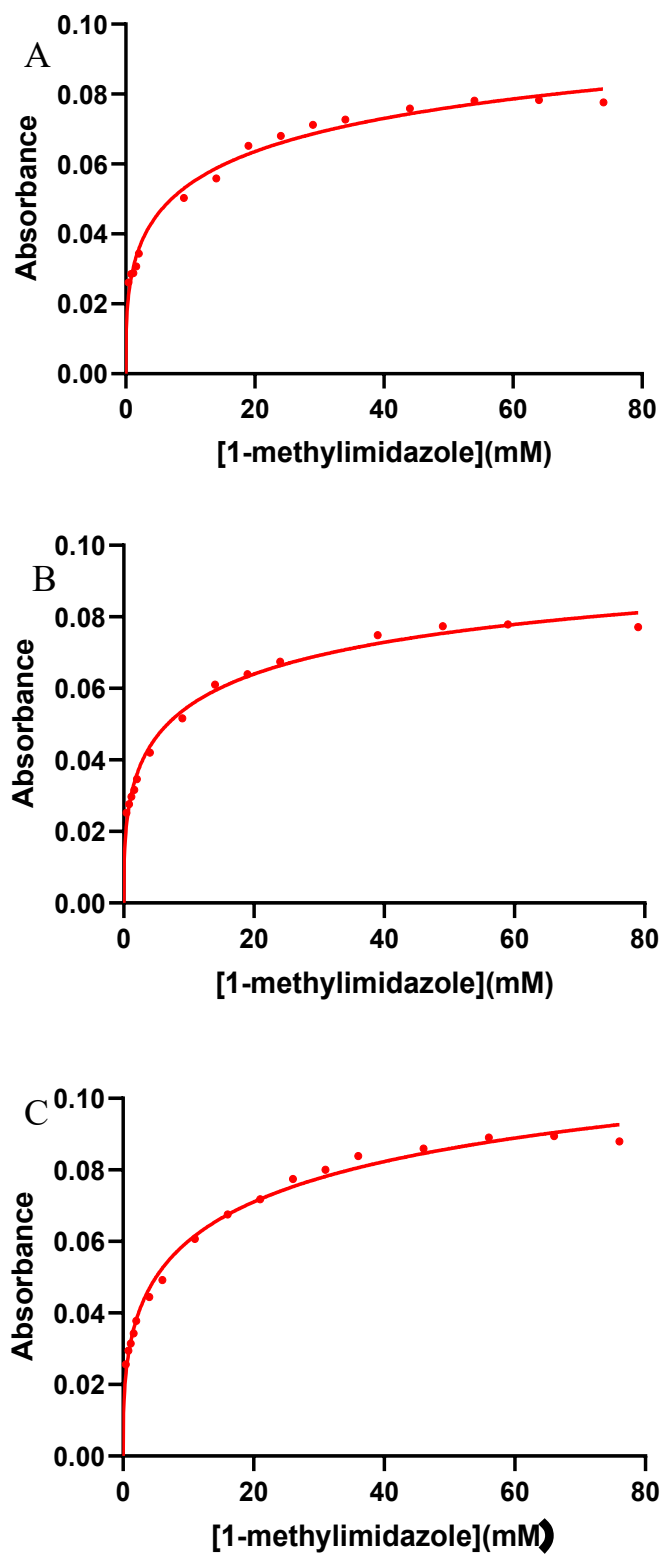


Figure 2.32. Triplicate metal Cobalt titrations with 1-methylimidazole. (A+B+C): 1-methylimidazole-dependent absorbance changed at 500 nm were monitored in the presence of 5 mM Co (II). The data was fitted to the specific binding and Hill slope equation.

2.5.2.3 Concentration of 1-butylimidazole used to synthesize octanol soluble Co (II) complex

1-butylimidazole was insoluble in buffer, so competition experiments could not be performed in buffer. Therefore, to find the most suitable concentration of 1-butylimidazole, Co (II)-N-Acetyl-L-cysteine methyl ester-1-butylimidazole complex was synthesized in the mixture of buffer and octanol, using 5 mM N-Acetyl-L-cysteine methyl ester, 5 mM Co (II) (the concentration used was roughly equal to K_d value for S-Co (II) coordination) and different concentration of 1-butylimidazole. According to the UV-Vis spectra for organic phase and aqueous phase (Figure 2.34-2.39), as the increasing of concentration of 1-butylimidazole used to synthesize the Co (II) complex, the absorbance at around 630 nm for CoS_2N_2 complex in organic phase increased. The absorbance at around 750 nm for CoS_4 complex in aqueous phase decreased when the concentration of 1-butylimidazole used increased, which meant Co (II) complex formed in buffer changed from CoS_4 to the mixture of Co (II) complex of other forms. When the concentration of 1-butylimidazole used was low, a small amount of Co (II) was coordinated with 1-butylimidazole and a small amount of the thiol ligands, forming CoS_2N_2 complex and partitioned to octanol, most of the Co (II) and thiol ligands tended to form CoS_4 complex in buffer. When the concentration of 1-butylimidazole used increased, more Co (II), thiol ligands tended to synthesize CoS_2N_2 complex with 1-butylimidazole and partitioned to octanol, the rest of Co (II) and thiol ligands formed CoS_4 complex in buffer. When the concentration of 1-butylimidazole was larger than 75 mM, most of 1-butylimidazole used and thiol ligands was coordinated to Co (II) to form CoS_2N_2 and migrated to octanol, Co (II) coordinated with a small amount of 1-butylimidazole and thiol ligands left in buffer to form a mixture of Co (II) complex in different form, may mostly include CoS_2N_2 and small amount of CoS_4 . The color of organic phase was blue (B) and aqueous phase was light green (A) (Figure 2.33). According to the UV-Vis spectra, 50 mM 1-butylimidazole was finally chosen.

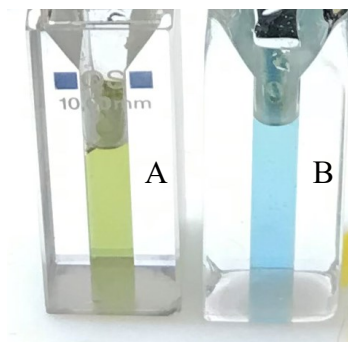


Figure 2.33. Color for Co (II) complex, (A) Aqueous phase (B) Organic phase. 5 mM N-Acetyl-L-cysteine methyl ester, 50 mM 1-butylimidazole, 5 mM Co (II), the mixture of octanol and 100 mM HEPES, pH 8 was used.

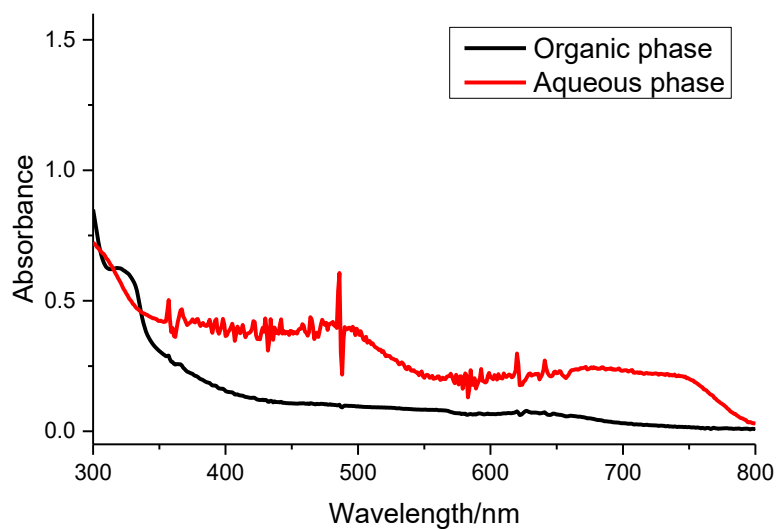


Figure 2.34. The UV-Vis spectra of Co (II)-N-Acetyl-L-cysteine methyl ester-1-butylimidazole complex, 5 mM N-Acetyl-L-cysteine methyl ester, 30 mM 1-butylimidazole, 5 mM Co (II), the mixture of octanol and 100 mM HEPES, pH 8 was used. The points (655, 0.065206) (656, 0.072496) (657, -0.01715) (658, 0.044466) of organic spectrum and (655, 0.284916) (656, 0.429155) (657, -0.10587) (658, 0.081929) of aqueous spectrum were deleted to smooth the spectra.

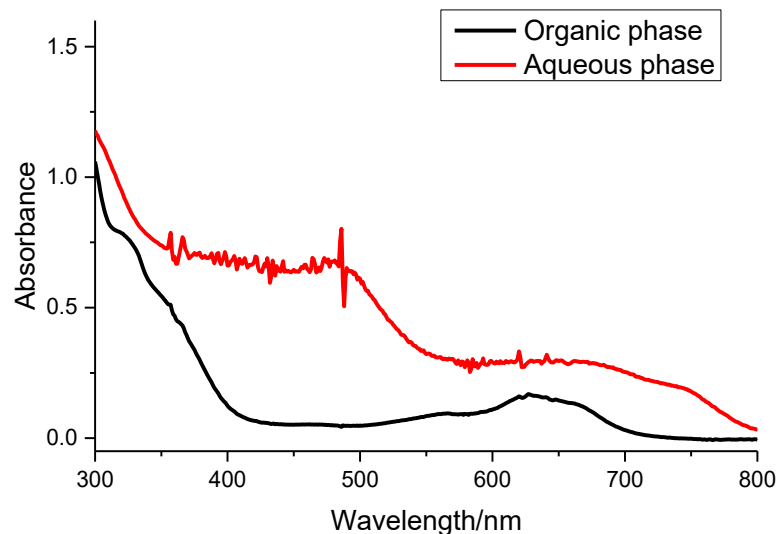


Figure 2.35. The UV-Vis spectra of Co (II)-N-Acetyl-L-cysteine methyl ester-1-butylimidazole complex, 5 mM N-Acetyl-L-cysteine methyl ester, 50 mM 1-butylimidazole, 5 mM Co (II), the mixture of octanol and 100 mM HEPES, pH 8 was used. The points (655, 0.320296) (656, 0.374375) (657, 0.078203) (658, 0.206754) of aqueous spectrum and (655, 0.14424) (656, 0. 0.148502) (657, 0.083562) (658,0.125221) of organic spectrum were deleted to smooth the spectra.

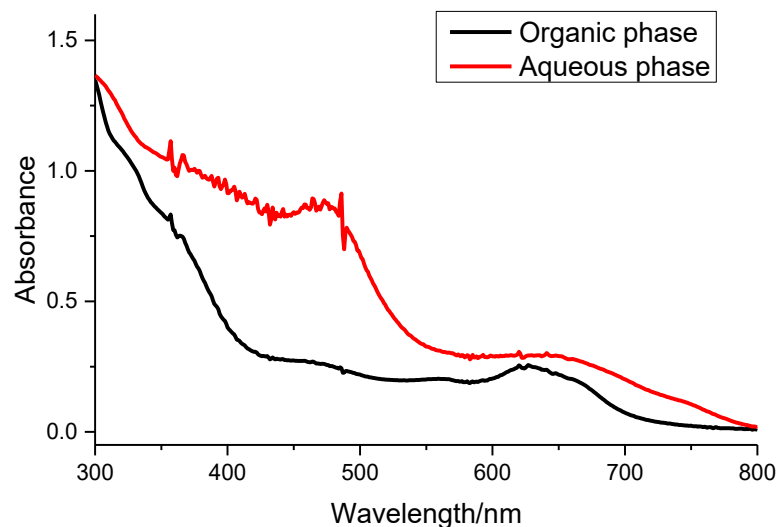


Figure 2.36: The UV-Vis spectra of Co (II)-N-Acetyl-L-cysteine methyl ester-1-butylimidazole complex, 5 mM N-Acetyl-L-cysteine methyl ester, 75 mM 1-butylimidazole, 5 mM Co (II), the mixture of octanol and 100 mM HEPES, pH 8 was used. The points (655, 0.293508) (656, 0.313011) (657, 0.183502) (658, 0.250647) of aqueous spectrum and (655, 0.222638) (656, 0.226716) (657, 0.138519) (658, 0.191624) of organic spectrum were deleted to smooth the spectra.

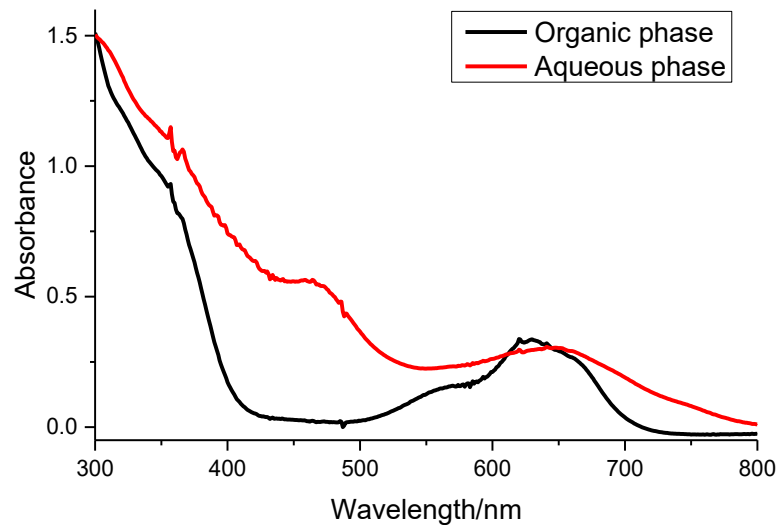


Figure 2.37. The UV-Vis spectra of Co (II)-N-Acetyl-L-cysteine methyl ester-1-butylimidazole complex, 5 mM N-Acetyl-L-cysteine methyl ester, 100 mM 1-butylimidazole, 5 mM Co (II), the mixture of octanol and 100 mM HEPES, pH 8 was used. The points (655, 0.30548) (656, 0.315799) (657, 0.232276) (658, 0.275661) of aqueous spectrum and (655, 0.280448) (656, 0.306195) (657, 0.18276) (658, 0.247228) of organic spectrum were deleted to smooth the spectra.

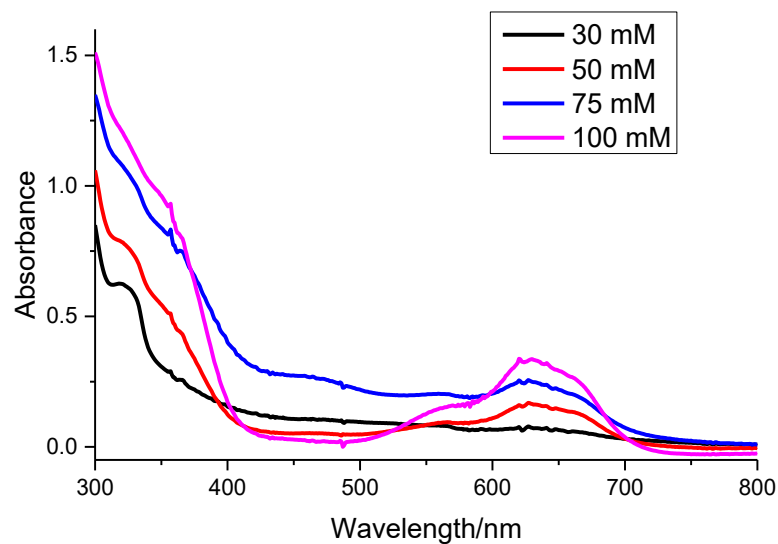


Figure 2.38. The UV-Vis spectra of Co (II)-N-Acetyl-L-cysteine methyl ester-1-butylimidazole complex in organic phase, 5 mM N-Acetyl-L-cysteine methyl ester, 5mM Co (II), 1-butylimidazole of various concentration, the mixture of octanol and 100 mM HEPES, pH 8 was used.

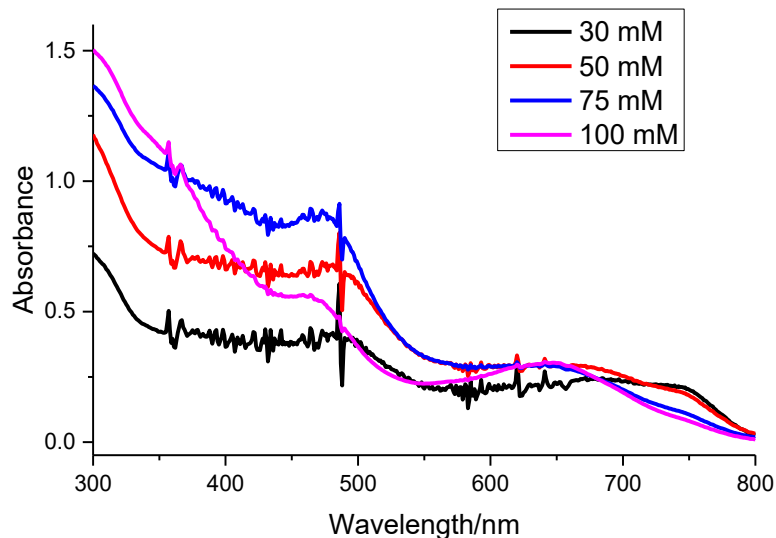


Figure 2.39. The UV-Vis spectra of Co (II)-N-Acetyl-L-cysteine methyl ester-1-butylimidazole complex in aqueous phase, 5 mM N-Acetyl-L-cysteine methyl ester, 5mM Co (II), 1-butylimidazole of various concentration, the mixture of octanol and 100 mM HEPES, pH 8 was used.

2.5.2.4 Concentration of 2-propanethiol used to synthesize octanol soluble Co (II) complex

The solubility of 2-propanethiol in buffer was low, so it was difficult to do the competition experiment of 2-propanethiol-Co (II) coordination in buffer. To find the most suitable concentration for 2-propanethiol to synthesize octanol soluble Co (II)-1-butylimidazole-2-propanethiol complex, such Co (II) complex was synthesized in the mixture of buffer and octanol, using 50 mM of 1-butylimidazole and 5 mM Co (II), and various concentration of 2-propanethiol. According to the UV-Vis spectra for organic phase and aqueous phase (Figure 2.41-2.47), in organic phase, the absorbance at around 630 nm for CoS_2N_2 complex increased when the concentration of 2-propanethiol was increased. In aqueous phase, the absorbance at around 500 nm indicated that some of the 1-butylimidazole was coordinated to Co (II) to form CoN_4 in buffer. Comparing with 1-butylimidazole, Co (II) showed a weaker binding affinity for 2-propanethiol-Co (II) coordination, so to synthesize CoS_2N_2 complex soluble in octanol, a high concentration of 2-propanethiol needed to be used. When the concentration of 2-propanethiol used was low (smaller than 50 mM), a small amount of CoS_2N_2 was synthesized in octanol by Co (II), 1-butylimidazole and 2-propanethiol used, most of

the Co (II) and 1-butylimidazole ligands tended to form CoN_4 complex in buffer. When the concentration of 2-propanethiol used was larger than 105 mM, a larger amount of CoS_2N_2 was synthesized in octanol and the rest of Co (II) and 1-butylimidazole tended to form CoN_4 complex in buffer. The color of the organic phase was blue (B) and the aqueous phase was light red (A) (Figure 2.40). According to the UV-Vis spectra, 161 mM 2-propanethiol was finally chosen.

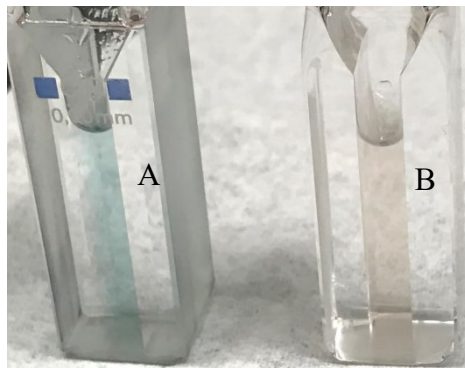


Figure 2.40. Color for Co (II) complex, (A) Organic phase (B) Aqueous phase. 161 mM 2-propanethiol, 50 mM 1-butylimidazole, 5 mM Co (II), the mixture of octanol and 100 mM HEPES, pH 8 was used.

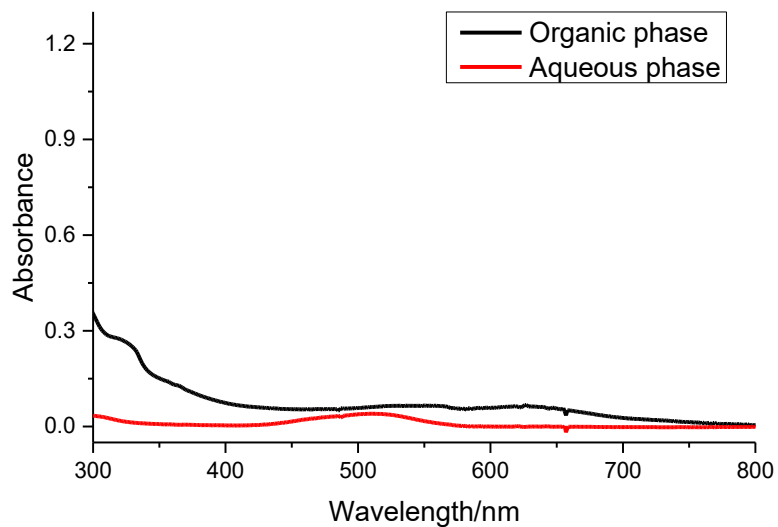


Figure 2.41. The UV-Vis spectra of Co (II)-2-propanethiol-1-butylimidazole complex, 50 mM 1-butylimidazole, 5 mM Co (II), 5 mM 2-propanethiol, the mixture of octanol and 100 mM HEPES, pH 8 was used.

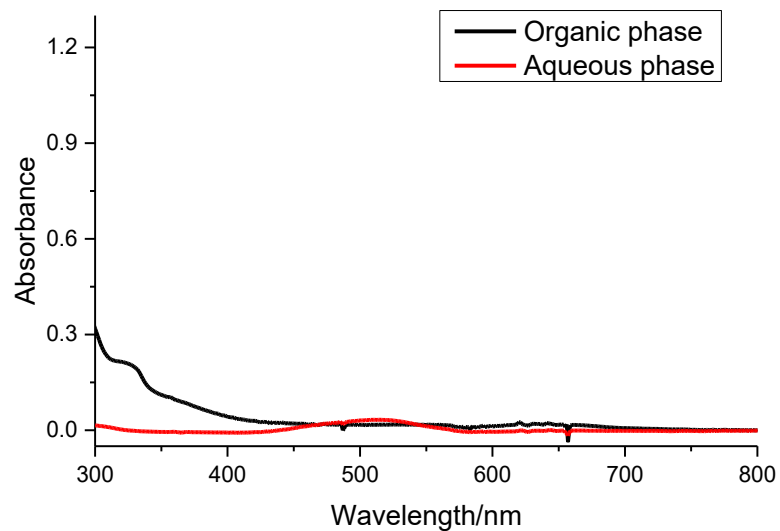


Figure 2.42. The UV-Vis spectra of Co (II)-2-propanethiol-1-butylimidazole complex, 50 mM 1-butylimidazole, 5 mM Co (II), 25 mM 2-propanethiol, the mixture of octanol and 100 mM HEPES, pH 8 was used.

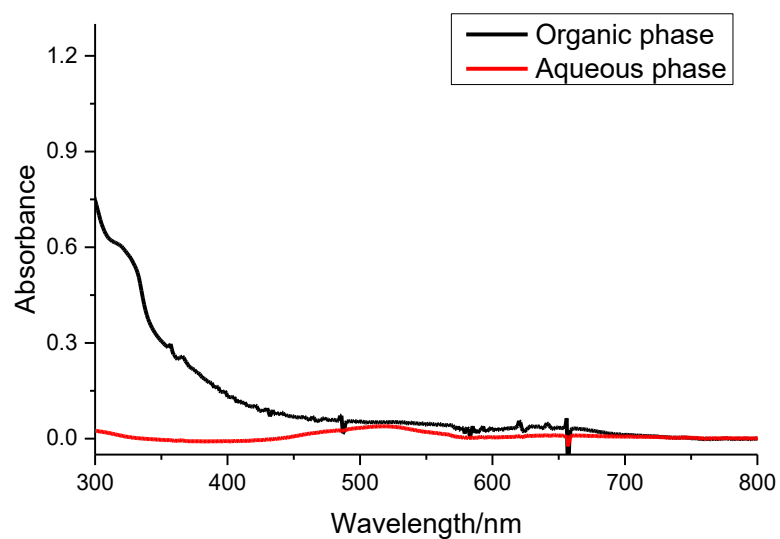


Figure 2.43. The UV-Vis spectra of Co (II)-2-propanethiol-1-butylimidazole complex, 50 mM 1-butylimidazole, 5 mM Co (II), 50 mM 2-propanethiol, the mixture of octanol and 100 mM HEPES, pH 8 was used.

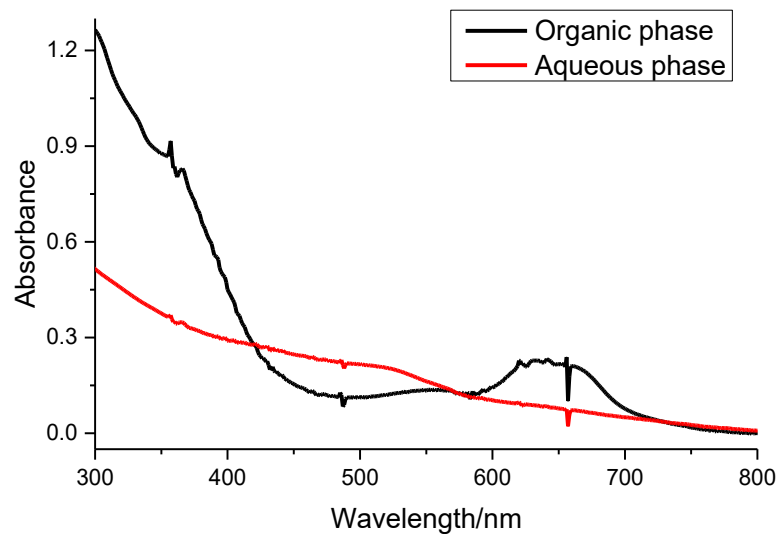


Figure 2.44. The UV-Vis spectra of Co (II)-2-propanethiol-1-butylimidazole complex, 50 mM 1-butylimidazole, 5 mM Co (II), 105 mM 2-propanethiol, the mixture of octanol and 100 mM HEPES, pH 8 was used.

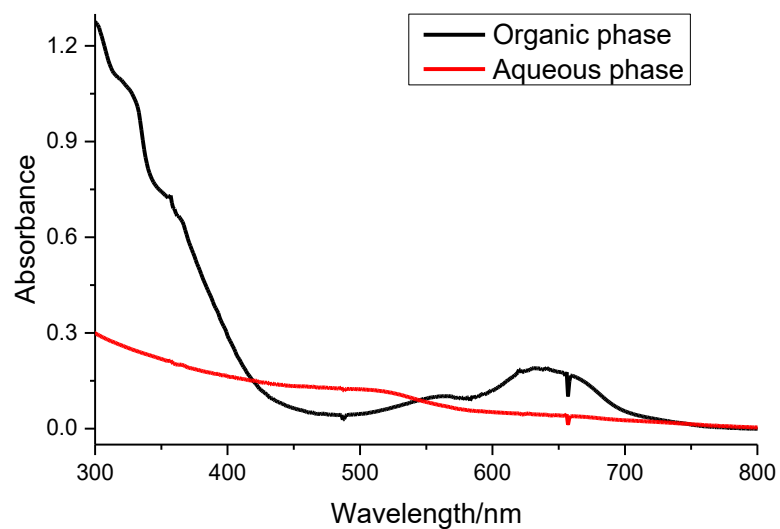


Figure 2.45. The UV-Vis spectra of Co (II)-2-propanethiol-1-butylimidazole complex, 50 mM 1-butylimidazole, 5 mM Co (II), 161 mM 2-propanethiol, the mixture of octanol and 100 mM HEPES, pH 8 was used.

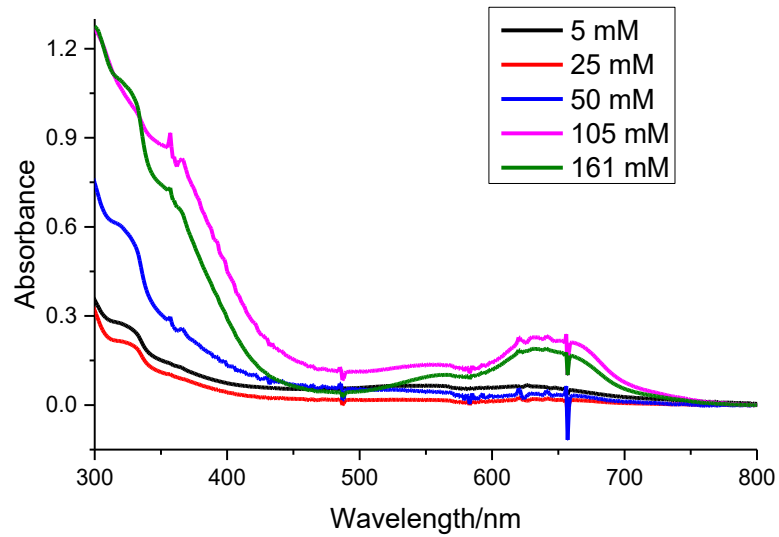


Figure 2.46. The UV-Vis spectra of Co (II)-2-propanethiol-1-butylimidazole complex in organic phase, 50 mM 1-butylimidazole, 5 mM Co (II), 2-propanethiol of various concentration, the mixture of octanol and 100 mM HEPES, pH 8 was used.

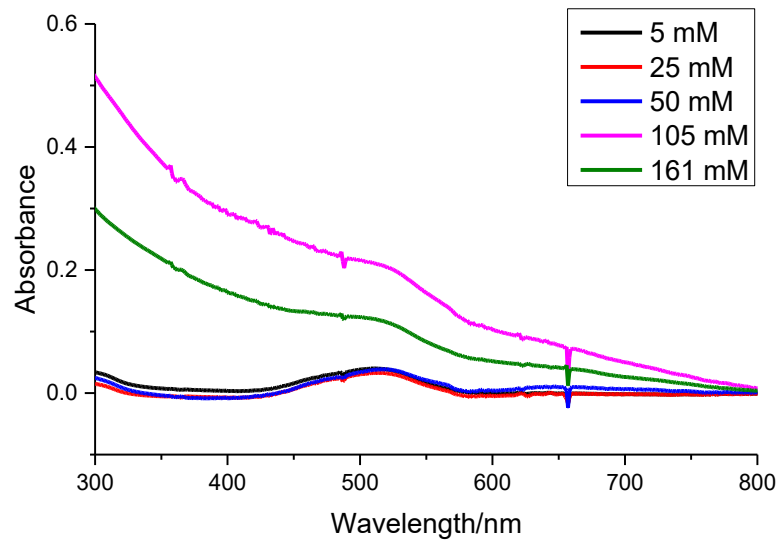


Figure 2.47. The UV-Vis spectra of Co (II)-2-propanethiol-1-butylimidazole complex in aqueous phase, 50 mM 1-butylimidazole, 5 mM Co (II), 2-propanethiol of various concentration, the mixture of octanol and 100 mM HEPES, pH 8 was used.

2.5.2.5 Co (II) complex was synthesized using the chosen concentration and concentration of K_d

Co (II)-2-propanethiol-1-methylimidazole complex was synthesized in the mixture of octanol and buffer, using 161 mM of 2-propanethiol (the concentration chosen) and 30 mM of 1-methylimidazole (equal to K_d for 1-methylimidazole-Co (II) coordination). The UV-Vis spectra of the organic phase indicated that the Co (II) complex could be soluble in octanol.

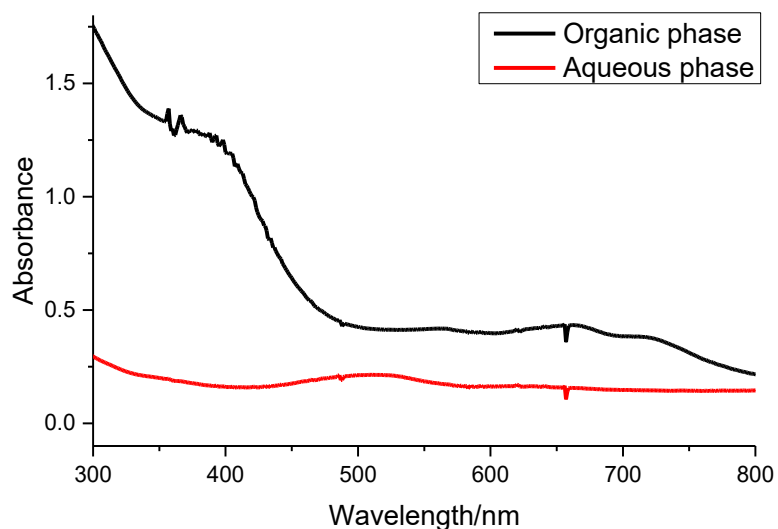


Figure 2.48. The UV-Vis spectra of Co (II)-2-propanethiol-1-methylimidazole complex, 161 mM 2-propanethiol, 5 mM Co (II), 30 mM 1-methylimidazole, and 100 mM HEPES, pH 8 was used.

Co (II)-N-Acetyl-L-cysteine methyl ester-1-methylimidazole complex was synthesized in the mixture of octanol and buffer, using 5 mM of N-Acetyl-L-cysteine methyl ester (K_d for N-Acetyl-L-cysteine methyl ester-Co (II) coordination) and 30 mM of 1-methylimidazole (K_d for 1-methylimidazole-Co (II) coordination). The UV-Vis spectra indicated that the Co (II) complex was not soluble in octanol and that the CoS_2N_4 was synthesized in buffer. This may be because the solubility of the Co (II) complex in octanol was also related to the solubility of ligands in octanol. 1-methylimidazole and N-Acetyl-L-cysteine methyl ester were all soluble in water, so even though the concentration of ligands used were the same as the K_d , the complex still could not dissolve in octanol.

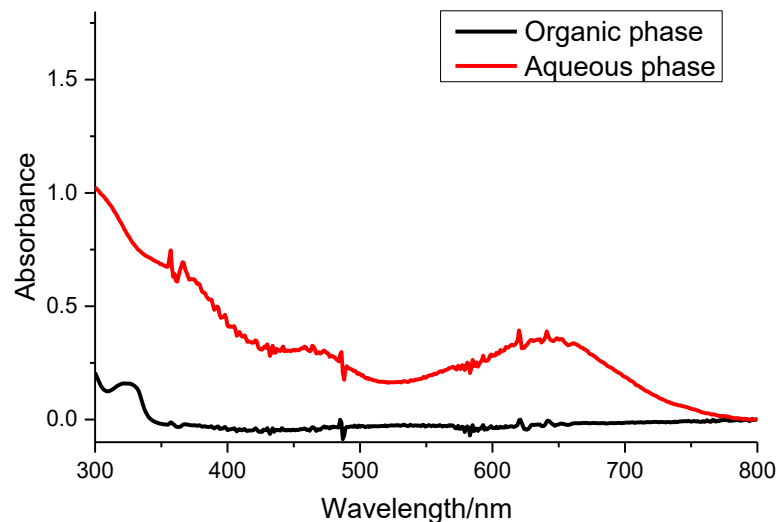


Figure 2.49. The UV-Vis spectra of Co (II)-N-Acetyl-L-Cysteine methyl ester-1-methylimidazole complex, 5 mM N-Acetyl-L-cysteine methyl ester, 30 mM 1-methylimidazole, 5 mM Co (II), the mixture of octanol and 100 mM HEPES, pH 8 was used. The points (655, 0.382825), (656, 0.474349), (657, 0.07969), and (658, 0.23741) of aqueous spectrum and (655, -0.01509), (656, 0.011846), (657, -0.16192), (658, -0.05812) of organic spectrum were deleted to smooth the spectrum.

2.5.3 Discussion

Co (II) showed different binding affinity to different ligands. To synthesize the Co (II) complex, if at least one of the two ligands used had a high solubility in octanol and the concentration of ligands was the same the K_d for ligand-Co (II) coordination, this synthesized Co (II) complex could be soluble in octanol. Additionally, using the concentration of ligands the same as K_d could make the complex synthesis comparable by using the same concentration for the same ligands to synthesize different complexes with different ligands (Chart 2).

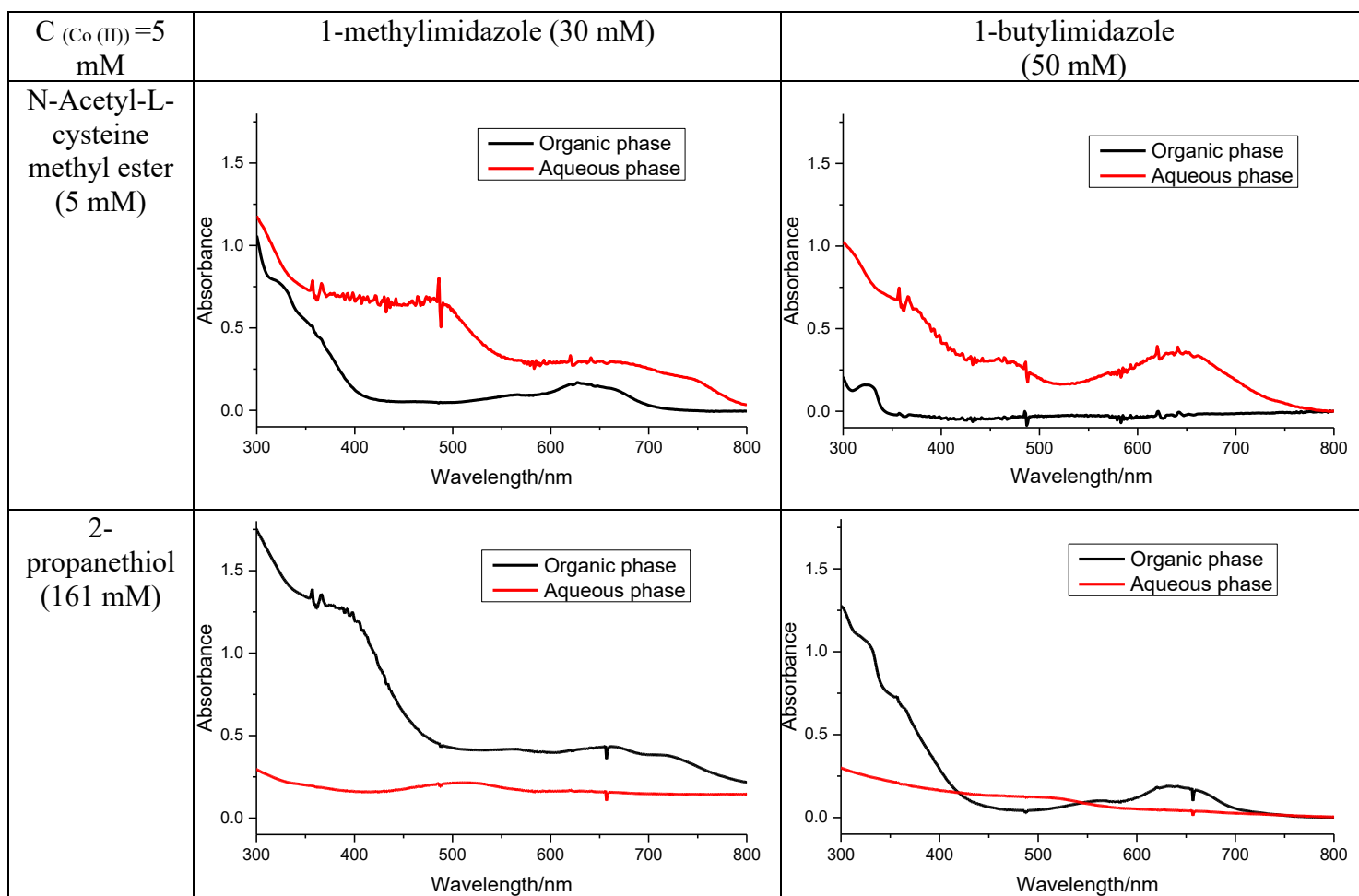


Table 2.2. The UV-Vis spectra of Co (II) complex synthesized in the mixture of octanol and buffer.

Chapter 3

Synthesis and characterization of Iron complex.

3.1 Introduction

To put the Iron (II) complex in the membrane of vesicles, the neutral Iron complex in which Fe (II) was coordinated with two thiol ligands and two imidazole ligands (FeS_2N_2) was aimed to be synthesized. FeS_2N_2 was firstly synthesized in HEPBS buffer in different conditions and evaluated by UV-Vis spectroscopy. Then FeS_2N_2 complex was synthesized in the mixture of octanol and buffer and its solubility in octanol could be indicated by the UV-Vis spectra of organic phase and aqueous phase. The Fe (II) complex that was soluble in octanol could be chosen to do a further study to be put in the membrane of vesicles. Different from the Cobalt complexes, the UV-Vis spectra of Fe (II) complexes are difficult to interpret in terms of the number of thiols coordinated with Fe (II), so we could not know the structure and the charge carried by Fe (II) complex synthesized. Therefore, we applied the same logic and conclusion of octanol soluble Co (II) complex synthesis to synthesize octanol soluble Fe (II) complex.

3.2 Synthesis and characterization of Fe (II)-thiol complex, Fe (II)-imidazole complex and Fe (II)-thiol-imidazole complex

3.2.1 Experimental plan

To find the best condition for the neutral Fe (II)-imidazole-thiol complex formation, the Fe (II) complex in which Fe (II) was coordinated with only thiol-containing ligands or imidazole ligands were firstly synthesized in different conditions and evaluated by means of UV-vis spectroscopy. Fe (II)-imidazole-thiol complex were then synthesized. According to the results of Co (II) complex, we chose thiol ligands including N-Acetyl-L-cysteine methyl ester and imidazole ligands including imidazole, 1-methylimidazole and 1-butylimidazole.

3.2.2 Experimental results

3.2.2.1 Fe (II)-N-Acetyl-L-cysteine methyl ester complex

Titration of N-Acetyl-L-cysteine methyl ester to 3 mM Fe (II) was performed in HEPBS at pH value of 8.8 in an anaerobic environment. The absorbance of the peaks at around 310 nm kept increasing, which indicated that Fe (II)-thiol complexes could be successfully synthesized (Figure 3.1, A.1-2).

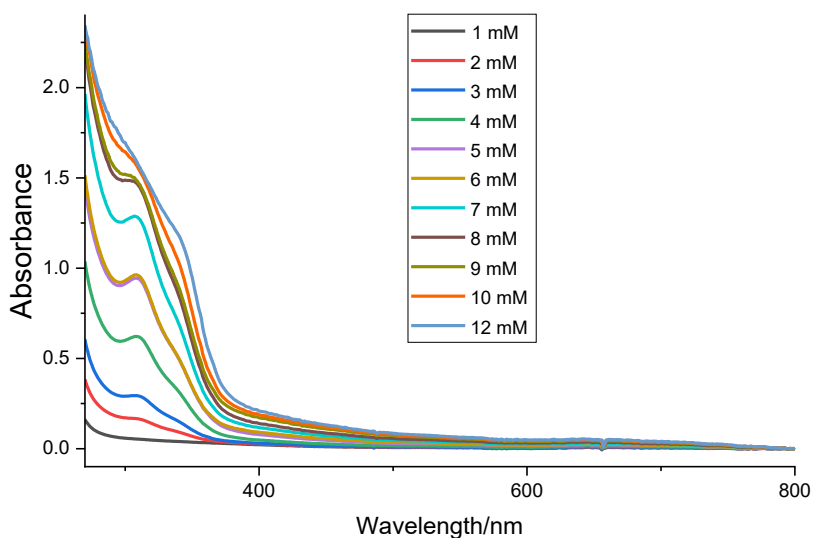


Figure 3.1. The UV-Vis spectra of Iron titrations with N-Acetyl-L-cysteine methyl ester. 3 mM Fe (II) and 100 mM HEPBS, pH 8.8 was used.

3.2.2.2 Fe (II)-1-butylimidazole complex

In anaerobic environments, we titrated 1-butylimidazole to 3 mM Fe (II) in HEPBS at pH value of 8.8, The concentration-dependent increase of absorbance at 370 nm was observed (Figure 3.2). The UV-Vis spectra indicated that Fe (II)-1-butylimidazole complex could be successfully synthesized.

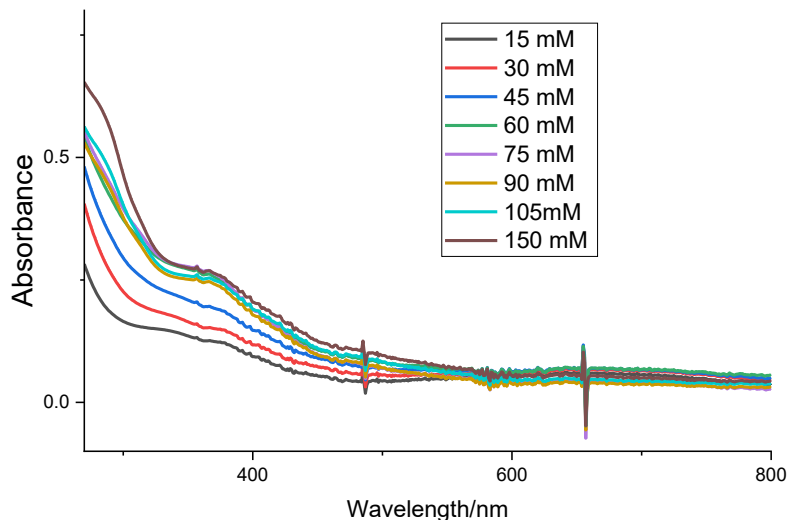


Figure 3.2. The UV-Vis spectra of Iron titrations with 1-butylimidazole. 0.7 mM Fe (II), and 100 mM HEPBS, pH 8.8 was used.

3.3 Synthesis and Characterization of Fe (II)-thiol-imidazole complex

3.3.1 Experimental plan

As what we did with Co (II) complex, to put the Fe (II) complex in the membrane of vesicles, the neutral Iron complex in which Fe (II) was coordinated with two thiol containing ligands and two imidazole ligands should be obtained. However, the number of thiols that were coordinated to Fe (II) could not be indicated by UV-Vis spectra. Therefore, in order to find the suitable condition for FeS₂N₂ complex synthesis and obtain the possible UV-Vis spectra indicated by FeS₂N₂, the titration of imidazole ligands to Fe (II)-N-Acetyl-L-cysteine methyl complex was performed in HEPBS buffer at pH value of 8.8 in anaerobic environment. During the titration, the changing of UV-Vis spectra as the imidazole adding to Fe (II)-N-Acetyl-L-cysteine methyl ester complex could be obtained. Imidazole, 1-methylimidazole and 1-butylimidazole were chosen as imidazole ligands.

3.3.2 Experimental results

The UV-Vis spectra (Figure 3.3-3.5 and A.3-A.4) indicated that, as imidazole ligands added to Fe (II)-N-Acetyl-L-cysteine methyl ester, the absorbance of the peak at 310 nm kept decreasing and a peak at 380 nm kept increasing. Figure 3.6-3.12 and showed the UV-Vis spectra for the titration of Fe (II) to 5 mM N-Acetyl-L-cysteine and different concentration of 1-butylimidazole, which showed how the UV-Vis spectra changed as the concentration of 1-butylimidazole ligands increased.

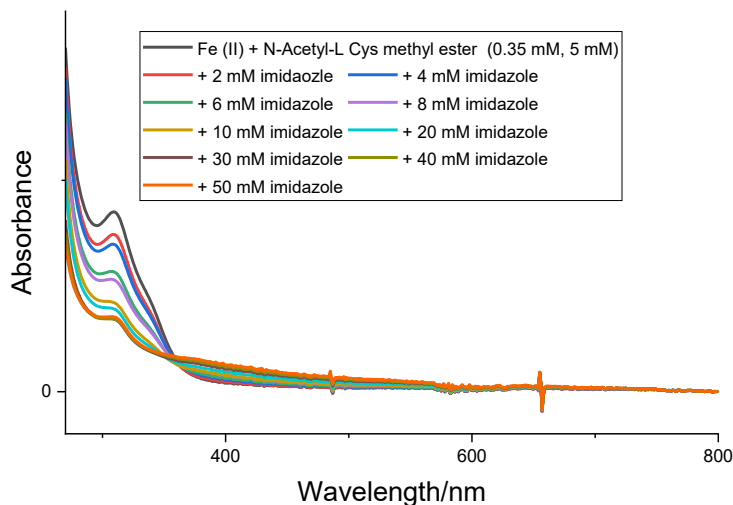


Figure 3.3. The UV-Vis spectra of Fe (II)-N-Acetyl-L-cysteine methyl ester complex titrations with imidazole. 0.35 mM Fe (II), 5 mM N-Acetyl-L-cysteine methyl ester, and 100 mM HEPBS, pH 8.8 was used.

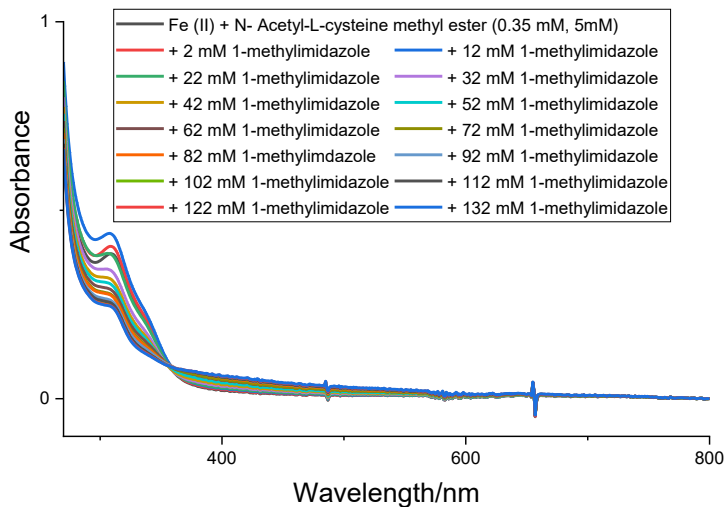


Figure 3.4. The UV-Vis spectra of Fe (II)- N-Acetyl-L-cysteine methyl ester complex titrations with 1-methylimidazole. 0.35 mM Fe (II), 5 mM N-Acetyl-L-cysteine methyl ester, and 100 mM HEPBS buffer, pH 8.8 was used.

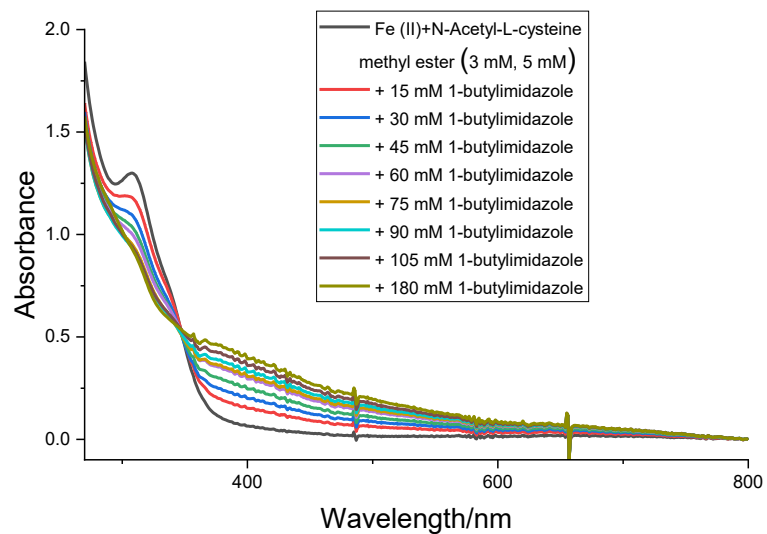


Figure 3.5. The UV-Vis spectra of Fe (II)-N-Acetyl-L-cysteine methyl ester complex titrations with 1-butylimidazole. 0.35 mM Fe (II), 5 mM N-Acetyl-L-cysteine methyl ester, and 100 mM HEPBS, pH 8.8 was used.

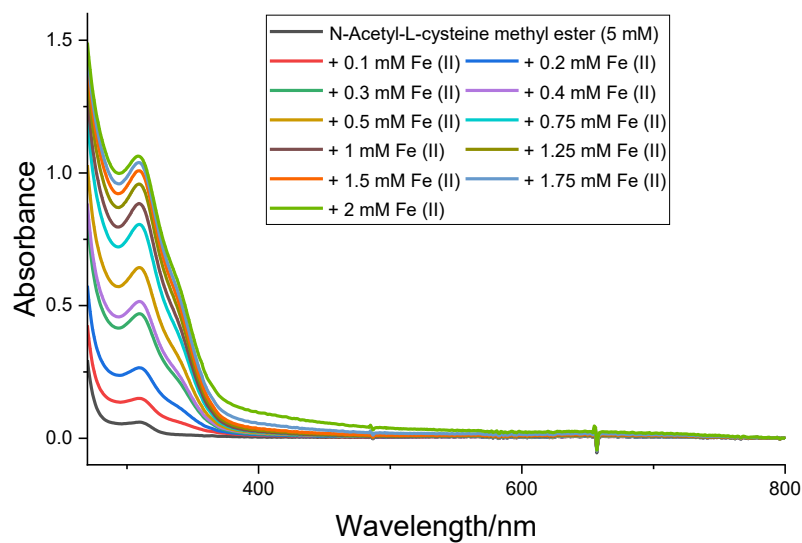


Figure 3.6. The UV-Vis spectra of N-Acetyl-L-cysteine methyl ester titrations with Fe (II). 5 mM N-Acetyl-L-cysteine methyl ester, 100 mM HEPBS, pH 8.8 was used.

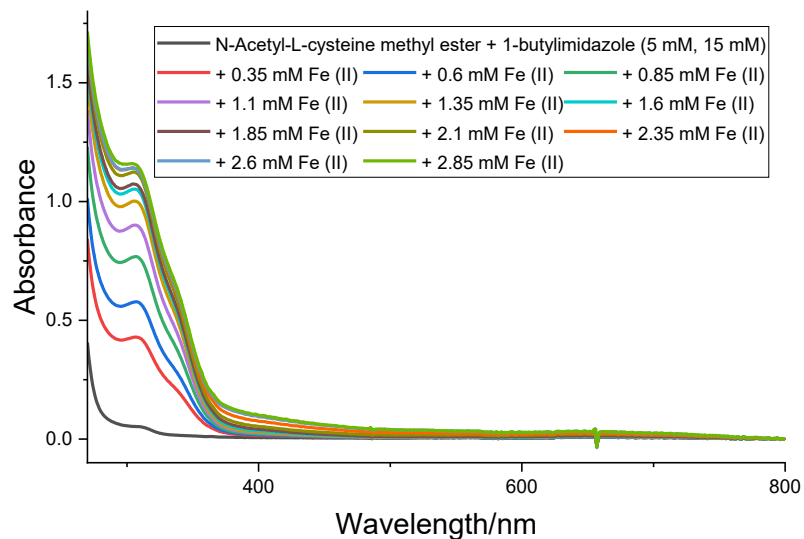


Figure 3.7. The UV-Vis spectra of N-Acetyl-L-cysteine methyl ester and 1-butylimidazole titrations with Fe (II). 5 mM N-Acetyl-L-cysteine methyl ester, 15 mM 1-butylimidazole and 100 mM HEPBS, pH 8.8 was used.

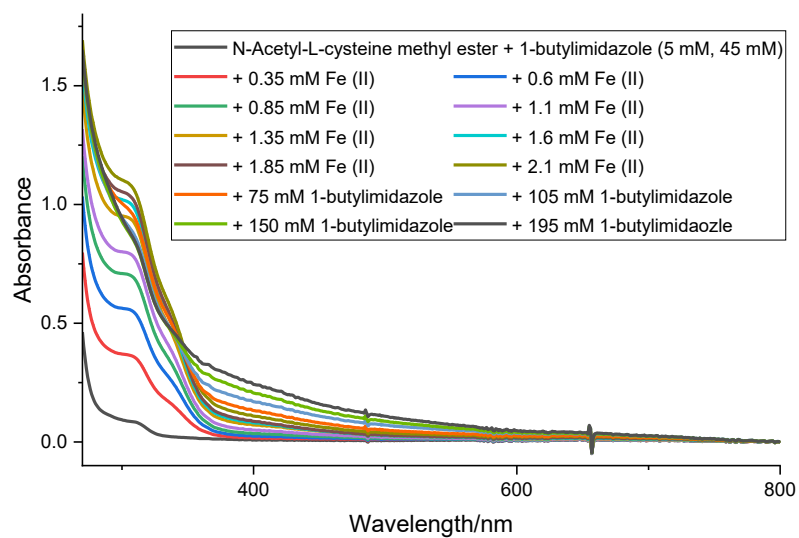


Figure 3.8. The UV-Vis spectra of N-Acetyl-L-cysteine methyl ester and 1-butylimidazole titrations with Fe (II). 5 mM N-Acetyl-L-cysteine methyl ester, 45 mM 1-butylimidazole and 100 mM HEPBS, pH 8.8 was used.

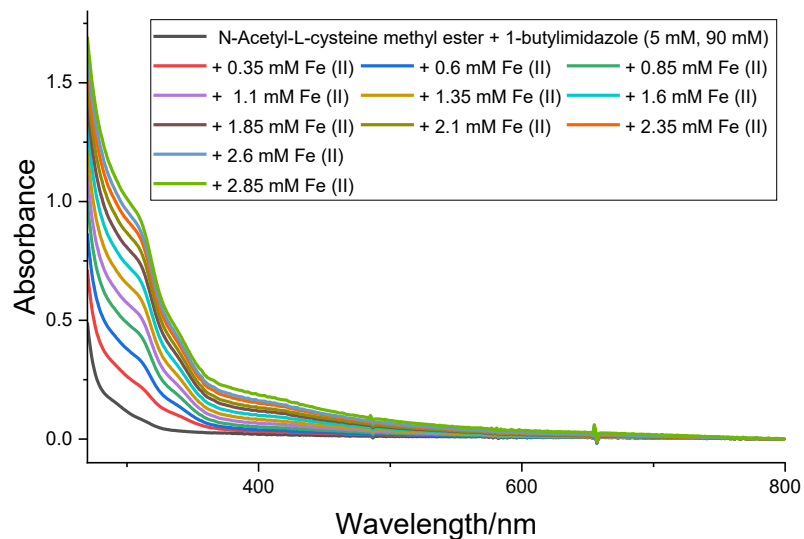


Figure 3.9. The UV-Vis spectra of N-Acetyl-L-cysteine methyl ester and 1-butylimidazole titrations with Fe (II). 5 mM N-Acetyl-L-cysteine methyl ester, 90 mM 1-butylimidazole and 100 mM HEPBS, pH 8.8 was used.

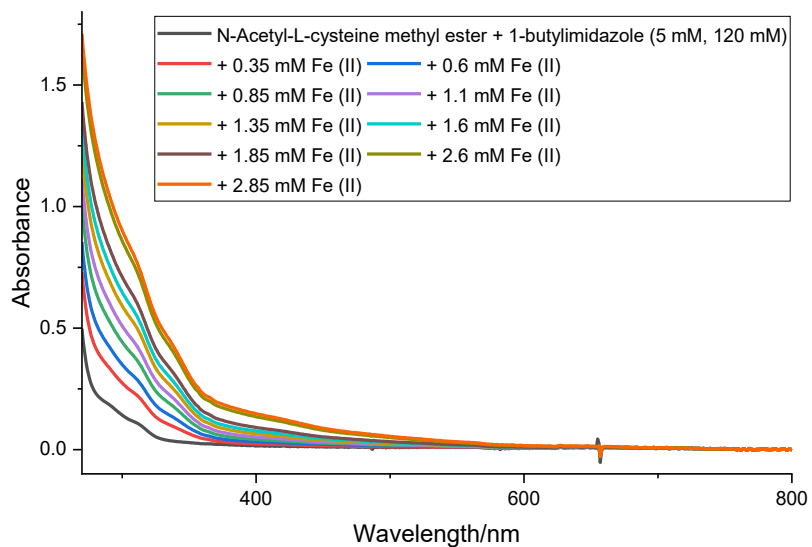


Figure 3.10. The UV-Vis spectra of N-Acetyl-L-cysteine methyl ester and 1-butylimidazole titrations with Fe (II). 5 mM N-Acetyl-L-cysteine methyl ester, 120 mM 1-butylimidazole and 100 mM HEPBS, pH 8.8 was used.

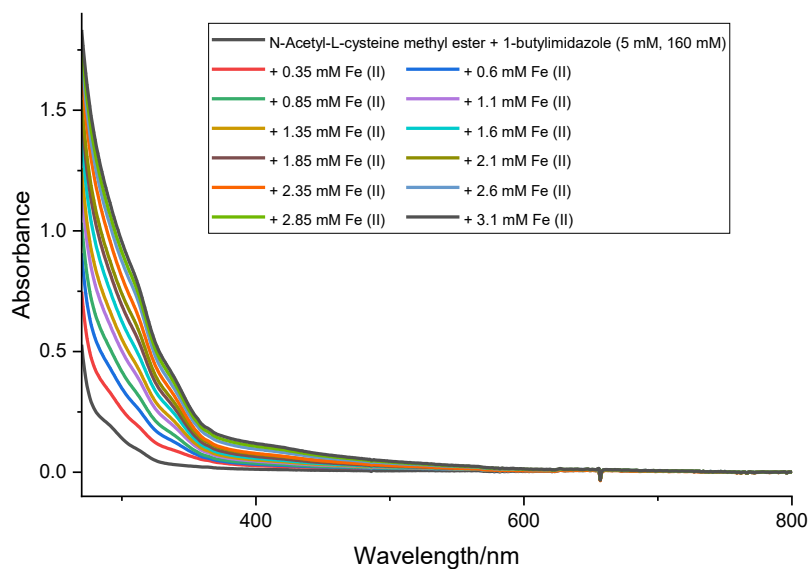


Figure 3.11. The UV-Vis spectra of N-Acetyl-L-cysteine methyl ester and 1-butylimidazole titrations with Fe (II). 5 mM N-Acetyl-L-cysteine methyl ester, 160 mM 1-butylimidazole and 100 mM HEPBS, pH 8.8 was used.

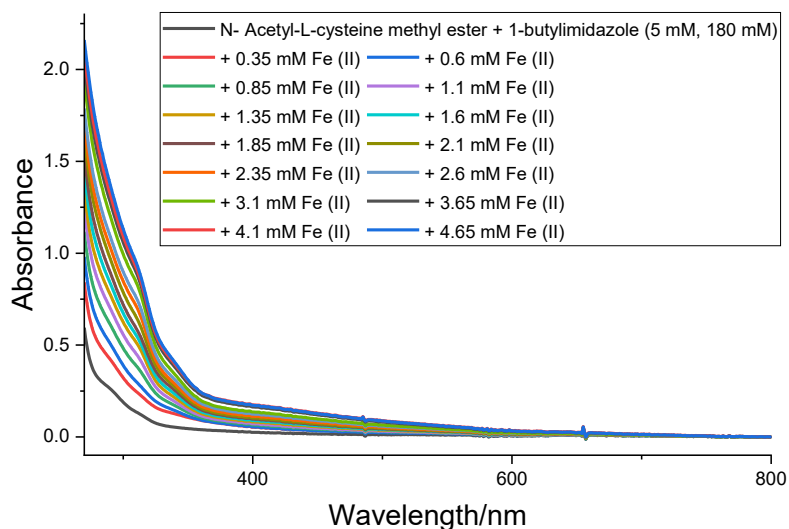


Figure 3.12. The UV-Vis spectra of N-Acetyl-L-cysteine methyl ester and 1-butylimidazole titrations with Fe (II). 5 mM N-Acetyl-L-cysteine methyl ester, 180 mM 1-butylimidazole and 100 mM HEPBS, pH 8.8 was used.

3.4 Synthesis of octanol soluble Fe (II) complex.

3.4.1 Experimental plan

The synthesis of octanol soluble Co (II) complexes indicated that the solubility of CoS_2N_2 was related to the solubility and concentration of the ligands. If the ligands with suitable solubility in octanol were used with concentrations equal to the K_d for ligand-Co (II) coordination, we could obtain an octanol soluble Co (II) complex. To get the octanol soluble Fe (II) complex, we choose 1-butylimidazole and N-Acetyl-L-cysteine as ligands. Then the K_d for S-Fe (II) coordination was calculated. 1-butylimidazole was insoluble in water, so it is difficult to do competition experiment in buffer. To get the suitable concentration of 1-butylimidazole to synthesize octanol soluble Fe (II) complex, Fe (II) complex was synthesized in a mixture of octanol and HEPBS buffer with different concentrations of 1-butylimidazole. According to the UV-Vis spectra, the suitable concentration of 1-butylimidazole could be obtained.

3.4.2 Experimental results

3.4.2.1 Binding affinity of N-Acetyl-L-cysteine methyl ester to Fe (II)

For N-Acetyl-L-cysteine methyl ester, the final value of K_d was calculated as the average of the three values obtained in each single set of experiments. In figure 2.19, results from saturation (direct titration) are shown. The results of the three replicates of N-acetyl-L-cysteine methyl ester titrations of 3 mM Iron (II) were indicated by Figure 3.13. The trend of absorbance monitored at 310 nm (FeS_4) against the concentration of N-Acetyl-L-cysteine methyl ester. For each of the three experiments was reported. Then these values were fit to the Hill equation to determine for each of the three cases the value of K_d . The final K_d for N-Acetyl-L-cysteine methyl ester-Fe (II) was 5 ± 1 mM (A. $K_d=3.965$ mM, $h=3.141$; B. $K_d=6.076$ mM, $h=2.026$; C. $K_d=5.012$ mM, $h=2.810$).

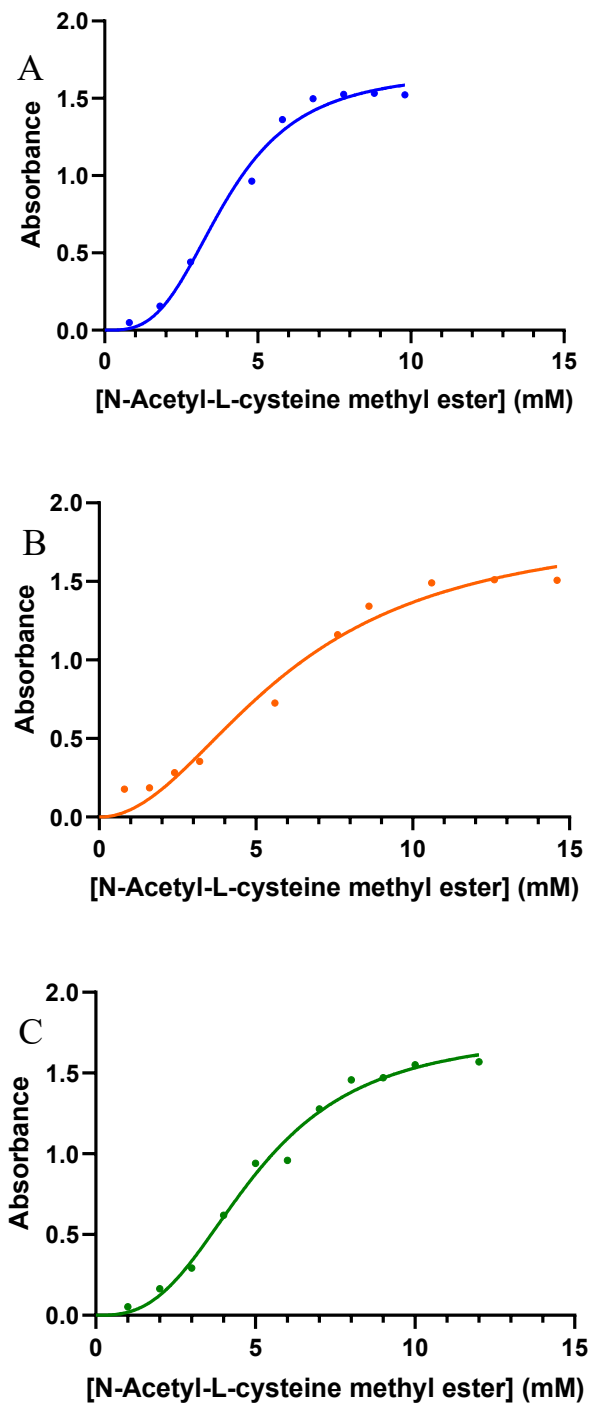


Figure 3.13. Triplicate Iron titrations with N-Acetyl-L-cysteine methyl ester. (A+B+C): N-Acetyl-L-cysteine methyl ester dependent absorbance changes at 310 nm were monitored in the presence of 3 mM Fe (II). The data was fitted to the specific binding and Hill slope equation.

3.4.2.2 Synthesis of octanol soluble Fe (II)-N-Acetyl-L-cysteine methyl ester-1-butyylimidazole complex.

Fe (II)-N-Acetyl-L-cysteine methyl ester-1-butyylimidazole complex was synthesized in the mixture of buffer and octanol, using 5 mM of N-Acetyl-L-cysteine methyl ester and 3 mM of Fe (II) (concentration was equal to K_d value for S-Fe (II) coordination), and different concentration of 1-butyylimidazole. According to the UV-Vis spectra for organic phase and aqueous phase (Figure 3.20), as the concentration of 1-butyylimidazole increased, a peak at around 350 nm in the organic phase started emerging and the absorbance of the peak kept increasing. The appearance of the peak could indicate the Fe (II) complex synthesized was soluble in octanol. When the concentration of 1-butyylimidazole was low (at 55 mM, Figure 3.14), the UV-Vis spectrum of the organic phase did not show a peak at 350 nm. After transferred from an anaerobic environment to an aerobic environment, the spectra did not change. It could indicate that there was no Iron complex in the octanol. When the concentration of 1-butyylimidazole was high (larger than 220 mM, Figure 3.16-3.19), the UV-Vis spectra of the organic phase showed a peak at around 350 nm, and when the Iron complex in octanol was transferred from an anaerobic environment to an aerobic environment, the peak at 350 nm disappeared. This meant that the Fe (II) complex in octanol could be oxidized. The oxidation of Fe (II) could also be shown by the color change of the organic phase. Figure 3.21 (A) shows the organic phase in an anaerobic environment. The color of the organic phase became yellow after transferred to an aerobic environment, consistent with the oxidation of the Fe (II) of the complex to Fe (III) (Figure 3.20 (B)). Based on the UV-Vis data, a suitable concentration of 1-butyylimidazole to synthesize an octanol soluble Fe (II) complex should be larger than 220 mM.

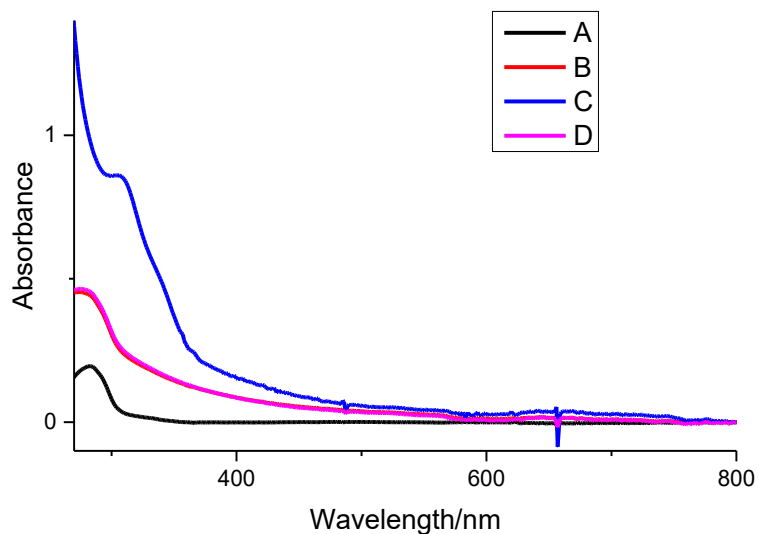


Figure 3.14. The UV-Vis spectra of Fe (II)-N-Acetyl-L-cysteine methyl ester-1-butylimidazole complex, 5 mM N-Acetyl-L-cysteine methyl ester, 55 mM 1-butylimidazole, 3 mM Fe (II), the mixture of octanol and 100 mM HEPBS, pH 8.8 was used. A: 55 mM 1-butylimidazole; B: spectra for organic phase; C: spectra for aqueous phase; D: spectra for organic phase after transferred to aerobic environment.

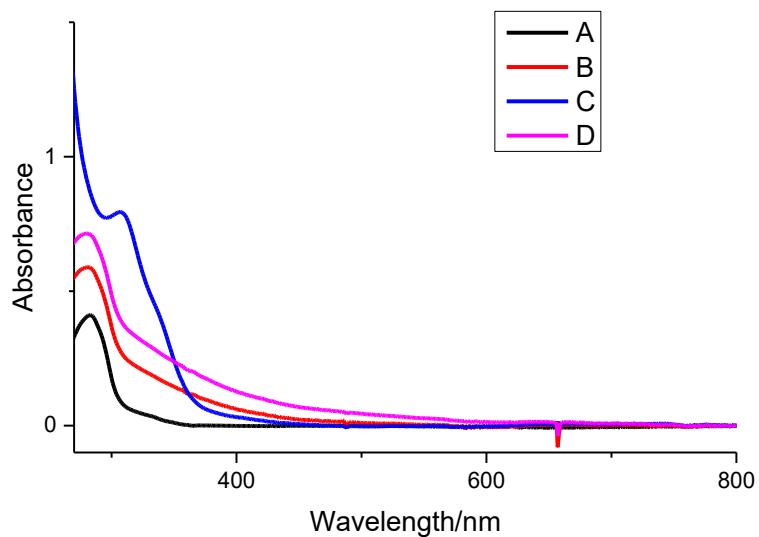


Figure 3.15. The UV-Vis spectra of Fe (II)-N-Acetyl-L-cysteine methyl ester-1-butylimidazole complex, 5 mM N-Acetyl-L-cysteine methyl ester, 110 mM 1-butylimidazole, 3 mM Fe (II), the mixture of octanol and 100 mM HEPBS, pH 8.8 was used. A: 110 mM 1-butylimidazole; B: spectra for organic phase; C: spectra for aqueous phase; D: spectra for organic phase after transferred to aerobic environment.

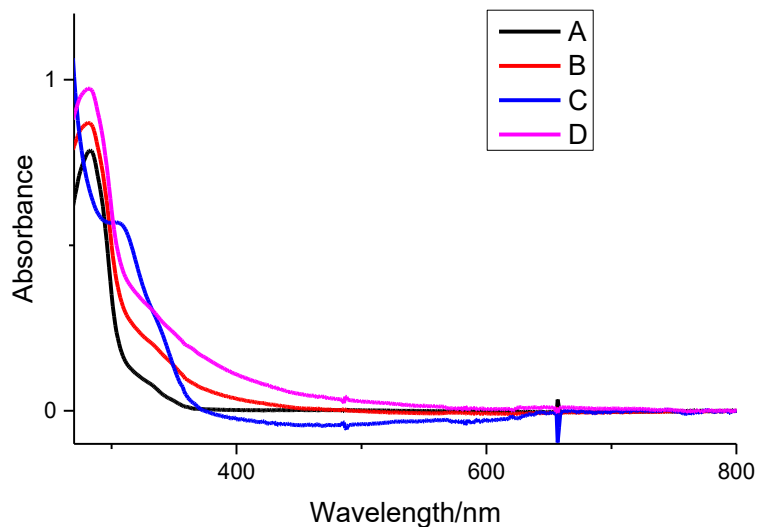


Figure 3.16. The UV-Vis spectra of Fe (II)-N-Acetyl-L-cysteine methyl ester-1-butylimidazole complex, 5 mM N-Acetyl-L-cysteine methyl ester, 220 mM 1-butylimidazole, 3 mM Fe (II), the mixture of octanol and 100 mM HEPBS, pH 8.8 was used. A: 220 mM 1-butylimidazole; B: spectra for organic phase; C: spectra for aqueous phase; D spectra for organic phase after transferred to aerobic environment.

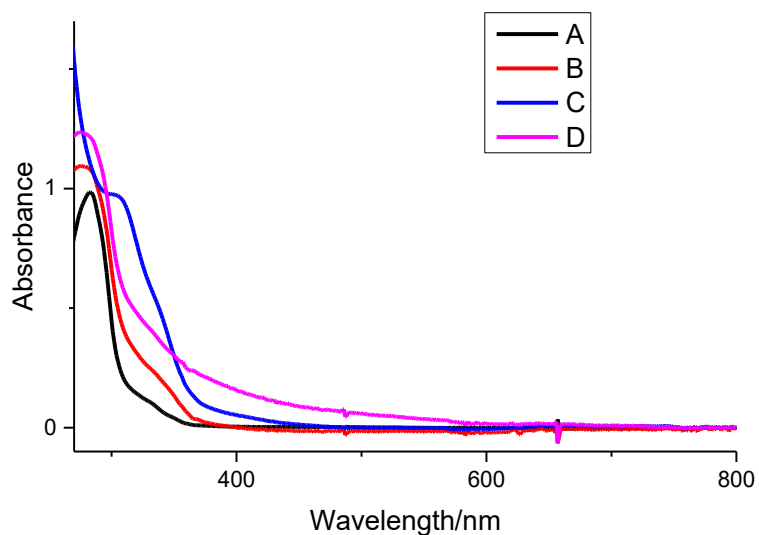


Figure 3.17. The UV-Vis spectra of Fe (II)-N-Acetyl-L-cysteine methyl ester-1-butylimidazole complex, 5 mM N-Acetyl-L-cysteine methyl ester, 275 mM 1-butylimidazole, 3 mM Fe (II), the mixture of octanol and 100 mM HEPBS, pH 8.8 was used. A: 275 mM 1-butylimidazole; B: spectra for organic phase; C: spectra for aqueous phase; D spectra for organic phase after transferred to aerobic environment.

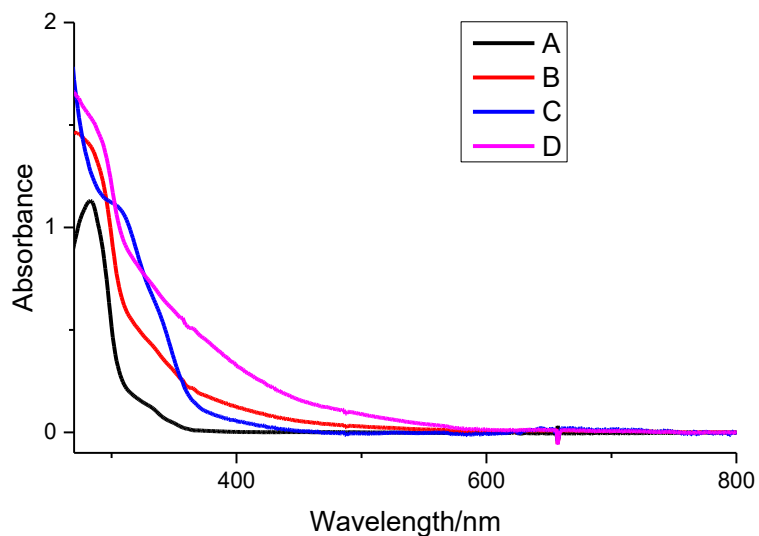


Figure 3.18. The UV-Vis spectra of Fe (II)-N-Acetyl-L-cysteine methyl ester-1-butylimidazole complex, 5 mM N-Acetyl-L-cysteine methyl ester, 330 mM 1-butylimidazole, 3 mM Fe (II), the mixture of octanol and 100 mM HEPBS, pH 8.8 was used. A: 330 mM 1-butylimidazole; B: spectra for organic phase; C: spectra for aqueous phase; D spectra for organic phase after transferred to aerobic environment.

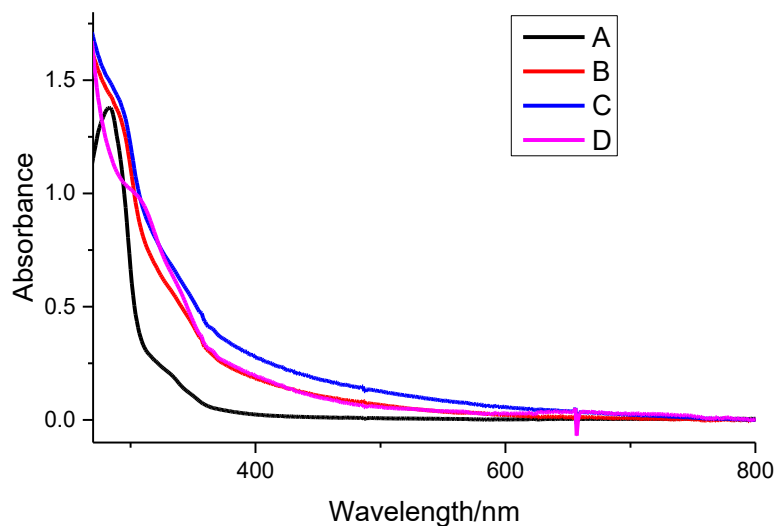


Figure 3.19. The UV-Vis spectra of Fe (II)-N-Acetyl-L-cysteine methyl ester-1-butylimidazole complex, 5 mM N-Acetyl-L-cysteine methyl ester, 375 mM 1-butylimidazole, 3 mM Fe (II), the mixture of octanol and 100 mM HEPBS, pH 8.8 was used. A: 375 mM 1-butylimidazole; B: spectra for organic phase; C: spectra for aqueous phase; D spectra for organic phase after transferred to aerobic environment.

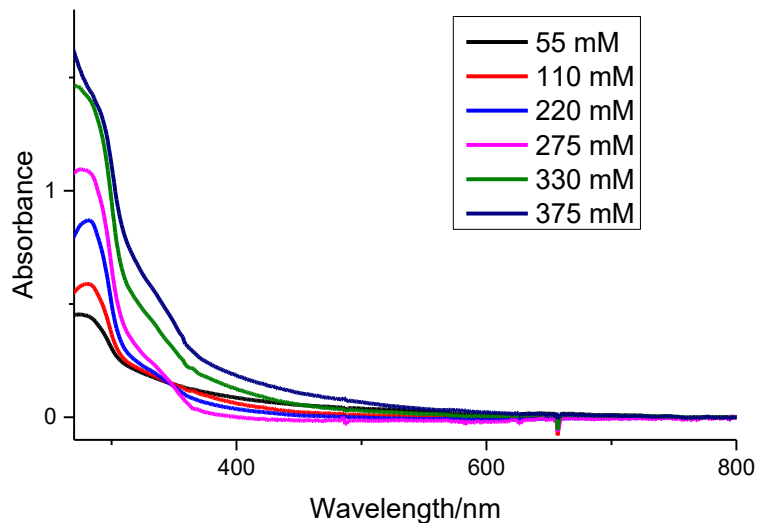


Figure 3.20. The UV-Vis spectra of Fe (II) complex in organic phase, 5 mM N-Acetyl-L-cysteine methyl ester, 3 mM Fe (II), 1-butylimidazole of various concentration, the mixture of octanol and 100 mM HEPBS, pH 8.8 was used.

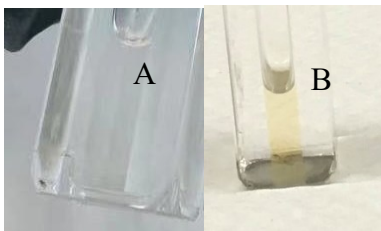


Figure 3.21. The color for Fe (II) complex, 5 mM N-Acetyl-L-cysteine methyl ester, 3 mM Fe (II), 275 mM 1-butylimidazole, the mixture of octanol and 100 mM HEPBS, pH 8.8 was used. (A) Fe (II) complex in organic phase in anaerobic condition (B) Fe (II) complex in organic phase after transferred to aerobic environment.

3.4.3 Discussion

According to the UV-Vis spectra, the octanol soluble Fe (II) complex could be synthesized with Fe (II), N-Acetyl-L-cysteine methyl ester of concentration equal to the K_d for S-Fe (II) coordination and 1-butylimidazole of concentration larger than 220 mM. This method could also be applied to the synthesis of the Fe (II) complex that was aimed to be put in the membrane of vesicles.

Chapter 4

POPC vesicles synthesis and metal complex in the membrane of vesicles.

4.1 Introduction

The membranes of POPC vesicles were used to provide an analogue of a protocellular membrane. It is important to emphasize that POPC is not generally considered to be prebiotically plausible. Metal complexes dissolved in octanol were synthesized and put in the membrane of vesicles. The metal complexes in the membrane could achieve the function of simple electron transfer across the membrane by donation and acceptance of the electrons.

4.2. POPC vesicles synthesis and put metal complex in the membrane of vesicles

4.2.1 Experimental plan

POPC Vesicles were synthesized in HEPBS buffer at pH 8.8, 1-butylimidazole, N-Acetyl-L-cysteine methyl ester and metal ion were then added to POPC vesicles samples. The concentration used was aimed to synthesize the octanol soluble complex. The metal complex could be synthesized, and the position of the metal complex could be detected by ^{31}P NMR spectroscopy.

4.2.2 Experimental results

4.2.2.1 ^{31}P NMR spectra of POPC vesicles with Co (II) complex

Figure 4.1 shows the ^{31}P NMR spectra of POPC vesicles, POPC vesicles with different ligands and POPC vesicles added with Co (II), and POPC vesicles with different Co (II) complexes. The result indicated that, comparing the ^{31}P NMR spectra of POPC vesicles, POPC vesicles + ligands and POPC vesicles + monoligand Co (II) complex, POPC vesicles + CoS_2N_2 complex had a broader peak, which meant that, CoS_2N_2

complex was the only chemicals that could migrate to and stay in the membrane of vesicles. The paramagnetism of Co (II) that partitioned to the POPC vesicle membranes shortened the relaxation times of the phosphorus centers of the phospholipids, which led to a decrease in the line-width of the corresponding resonance.

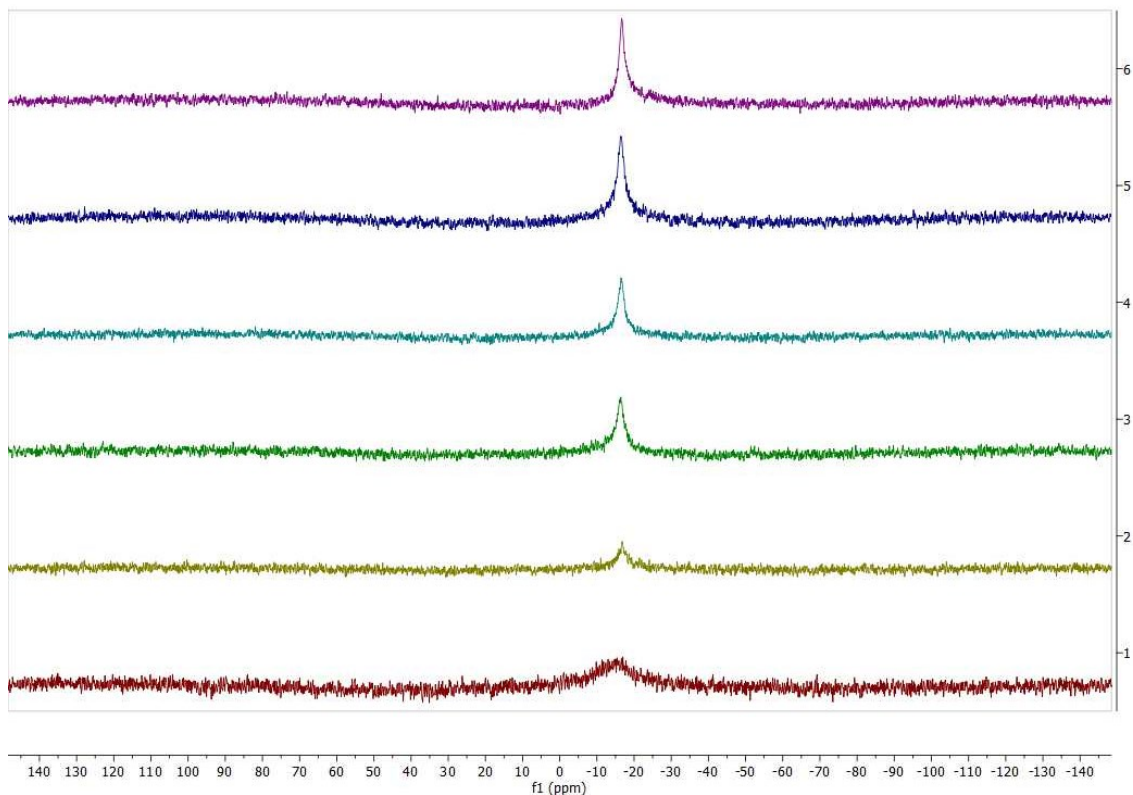


Figure 4.1. NMR spectra of POPC vesicles with different chemicals: 1. POPC vesicles (25 mM) + Co (II)-1-butylimidazole-N-Acetyl-L-cysteine methyl ester complex; 2. POPC vesicles (25 mM) + Co (II)-1-butylimidazole complex; 3. POPC vesicles (25 mM) + Co (II)-N-Acetyl-L-cysteine methyl ester complex; 4. POPC vesicles (25 mM) + Co (II)-EDTA complex; 5. POPC vesicles (25 mM) + Co (II); 6. POPC vesicles (25 mM).

4.2.2.2 ^{31}P NMR spectra of POPC vesicles with Fe (II) complex

Figure 4.2 indicated that, comparing to the ^{31}P NMR spectra of POPC vesicles, POPC vesicles + ligands and POPC vesicles + monoligand Fe (II) complex, POPC vesicles + Fe (II)-thiol-imidazole complex had a broader peak. The phosphorus resonance line of POPC molecules of NMR spectra could be broadened by the large amount of paramagnetism Fe (II) ions added surrounding the POPC molecules, which could indicate that the metal complex successfully partitioned to the membrane of the vesicles. Comparing to the POPC vesicles, POPC vesicles added with Fe (II) and POPC vesicles

added with Fe (II)-N-Acetyl-L-cysteine methyl ester complex, POPC vesicles added with Fe (II)-N-Acetyl-L-cysteine methyl ester-1-butylimidazole complex had a broader peak. Comparing with the Fe (II) ions of Fe (II) complex that dissolved in aqueous solution and could move freely outside the POPC vesicle membranes, Fe (II) ions of neutral Fe (II) complex partitioned to and fixed in the membrane of vesicles was closer to the phosphorus atom of POPC molecules. The unpaired electrons of Fe (II) close to the phosphorus of the lipid led to increased relaxation and thus broadened linewidths. POPC vesicles added with Fe (II) ions and Fe (II)-1-butylimidazole complex also showed line broadening. This may reflect oxidation of Fe (II) to Fe (III) and the binding of free Fe (III) to the phosphates of the headgroup of POPC.

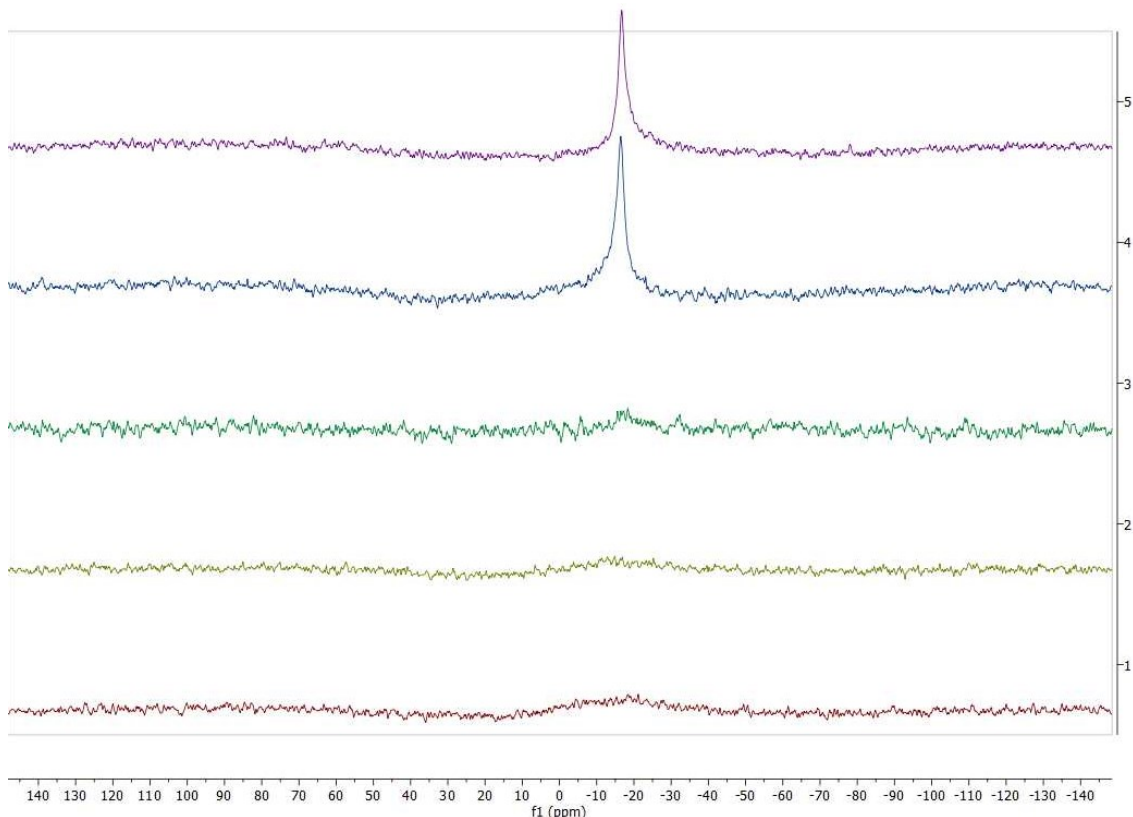


Figure 4.2. NMR spectra of POPC vesicles with different chemicals: 1. POPC vesicles (25 mM); 2. POPC vesicles (25 mM) + Fe (II)-N-Acetyl-L-cysteine methyl ester complex; 3. POPC vesicles (25 mM) + Fe (II); 4. POPC vesicles (25 mM) + Fe (II)-1-butylimidazole complex; 5. POPC vesicles (25 mM) + Fe (II)-1-butylimidazole-N-Acetyl-L-cysteine methyl ester complex.

4.3 Discussion

POPC vesicles were first formed in buffered aqueous solution, then after adding 1-butylimidazole, N-Acetyl-L-cysteine methyl ester and metal ions to the POPC vesicle samples, metal complexes were synthesized in aqueous solution. Just like the metal complexes above that could migrate from buffer to octanol, these octanol-soluble metal complexes could migrate from the buffered aqueous solution to the membrane of the vesicles and stay inside the membrane. The broadened phosphorus resonance line of POPC molecules on NMR spectra could indicate that we successfully put the paramagnetic metal complex in the membrane of the vesicles.

Chapter 5

Materials and Methods

5.1 Materials

All reagents were from Sigma-Aldrich and used without any further purification. The Milli-Q purified water was distilled under controlled nitrogen flow to deoxygenate the solvent. Schlenk lines and Schlenk glassware were used under controlled nitrogen atmosphere to obtain the metal Iron and ligands solutions. Hamilton gastight syringes were used to inject reagents or solutions into anaerobic sealed quartz cuvettes with a rubber septum for UV-Vis detection, or 5 mm NMR tubes used for ^{31}P NMR. Parafilm was used to wrap around the caps of the cuvettes or NMR tubes to seal the system. Orion Star A211 pH meter and ATC Probes from Thermo Scientific were used to measure the pH of solution. 5 mM NaOH and 3 mM HCl were used for pH adjustment.

5.2 Co (II) complex synthesis and Fe (II) complex synthesis

HEPES and HEPBS buffer were prepared by deoxygenated water in glass vials under anaerobic conditions. Ligands and metal ion solutions were mixed in buffer or mixture of buffer and octanol in a glass vial under anaerobic conditions.

5.3 POPC Vesicles Synthesis

POPC Vesicles: 25 mM POPC (1-palmitoyl-2-oleoyl-sn-glycero-3-phosphocholine) were prepared by thin-film rehydration using HEPBS buffer at pH 8.8. Samples were briefly vortexed, and then tumbled at room temperature overnight.

5.4 UV-Visible Absorption Spectroscopy

Samples were prepared under anaerobic condition and transferred to sealed quartz cuvettes (path length = 0.5 cm). UV-Visible absorption spectra of sample were collected using Agilent Cary 3500 UV-Vis spectrometer and Spectrophotometer, Hewlett Packard 8453. (integration = 0.02 s, interval = 1 nm).

5.5 Saturation Binding Assay

Ligands were injected into the cuvette to titrate 1 mL of an aqueous solution containing metal salt solution (FeCl_2 , $\text{CoCl}_2 \cdot 6\text{H}_2\text{O}$) at buffer (pH=8 HEPES for Co (II) and pH=8.8 HEPBS for Fe (II)). UV-Vis spectra were collected upon each addition and absorbance values were monitored at a fixed wavelength (750 nm for Co (II)-thiol coordination, 500 nm for Co (II)-imidazole, and 310 nm for Fe (II)-thiol coordination) until no changes were observed.

5.6 Determination of K_d

K_d values were calculated by GraphPad Prism v. 6.00 (GraphPad Software, La Jolla California USA) for Windows and then fitting the absorbance data to the equation:

$$Y = \frac{B_{\max} \times x^h}{K_d^h + x^h}$$

B_{\max} is the absorbance at saturation, x is the concentration, and h is the Hill slope.

5.7 ^{31}P NMR

^{31}P NMR spectra were acquired at room temperature by using Agilent/Varian DD2 MR two channel 400 MHz spectrometer. POPC vesicles sample were prepared into anaerobic sealed 5 mm NMR tubes.

Chapter 6

Conclusion and Future Work

Life relies on membranes, electron transfer reactions and proton-gradients. To explore if electron transfer within and proton gradients across a lipid membrane could be achieved with simple, prebiotically plausible components, we synthesized model prebiotic neutral metal complexes which partitioned to the membranes of lipid vesicles. These metal complexes were redox active and should be capable of participating in an electron transport chain.

Different thiol ligands and imidazole ligands were first used to synthesize Co (II) complexes in water-octanol mixtures. Octanol was used to mimic the lipid membrane of the vesicles. The solubility of the Co (II) complexes in octanol was measured by UV-Vis spectroscopy. The titration of different ligands to Co (II) was performed and the concentration of ligands equal to K_d was used to synthesize Co (II) complexes soluble in octanol. According to the UV-Vis spectra, the ligands and the logic of concentration of ligands used for the synthesis of octanol soluble metal complexes synthesis were finally determined. If at least one of the two ligands used had a high solubility in octanol and the concentration of ligands was equal to the value of K_d for ligand-Co (II) coordination, the synthesized Co (II) complex was soluble in octanol.

1-butylimidazole and N-Acetyl-L-cysteine methyl ester were then selected as the most suitable ligands to synthesize the octanol-soluble Fe (II) complex. The concentration of ligands and Fe (II) equal to the K_d of Co (II)-thiol coordination was used and the concentration of 1-butylimidazole was determined by comparing the UV-Vis spectra of Fe (II)-complex synthesized by Fe (II), N-Acetyl-L-cysteine methyl ester and different concentration of 1-butylimidazole. Metal complexes that were soluble in octanol were then synthesized in the membrane of POPC vesicles. The state of metal complex and if the metal complex could migrate to the membrane of vesicles could be detected by ^{31}P NMR spectra. Adding paramagnetic metal ions that partition to the POPC membrane leads to the broadening of the ^{31}P peaks. In the future, the relationship

between Log P of ligands and the octanol-water coefficient of Co (II) complex and Fe (II) complex could be further studied by synthesizing different complex and testing its solubility in octanol, in which different ligands including small peptides or organic compound could be tried. Based on the logic studied, metallopeptides and metal complex with a high tendency to be partitioned to octanol could be synthesized and then added to the membrane of lipid vesicles. The formation of lipid vesicles could be confirmed by visualization by fluorescence microscopy. How the metal complex accepts and donates electrons to achieve electron transfer and the generation of a proton gradient could be firstly studied in octanol-water system. The metal complex could be firstly synthesized and partitioned to octanol, the electron acceptor could then be added to the aqueous phase of octanol-water system. After shaking and reacting, the change of state of electron acceptor in aqueous phase could be tested, which would further help us to understand how the metal complex in octanol donates or accepts electrons. Subsequently, electron transfer could be studied within the membranes of lipid vesicles by NMR spectroscopy.

References

1. Brack, A. From the origin of life on Earth to life in the Universe. *Lectures in Astrobiology*, **2005**, *1*, 3–21.
2. Spontaneous Generation. <https://www.encyclopedia.com/science-and-technology/biology-and-genetics/biology-general/spontaneous-generation>.
3. Fry I. Emergence of life on earth: a historical and scientific overview. Rutgers University Press: USA, 2000.
4. Miller, S. L. The production of amino acids under possible primitive Earth conditions. *Science* **1953**, *117*, 528–529.
5. Lopez, A., and Fiore, M. Investigating Prebiotic Protocells for a Comprehensive Understanding of the Origins of Life: A Prebiotic Systems Chemistry Perspective. *Life (Basel)* **2019**, *9*, 49.
6. Sleep, N. The Hadean-Archaean Environment. *Cold Spring Harb. Perspect. Biol* **2010**, *2*, a002527.
7. Schrum, J.P., Zhu, T.F., Szostak, J.W. The Origins of Cellular Life Jason P. Schrum. *Cold Spring Harb Perspect Biol* **2010**, *2*, a002212.
8. Monnard, P.-A., and Walde, P. Current Ideas about Prebiological Compartmentalization. *Life* **2015**, *5*, 1239–1263.
9. Robinson, B. History of Biology: Cell Theory and Cell Structure. *Advameg, Inc* **2014**, Retrieved 17.
10. Weis, R.M., and McConnell, H.M. Two-dimensional chiral crystals of phospholipid. *Nature* **1984**, *310*, 47–49.
11. Deamer, D. The Role of Lipid Membranes in Life's Origin. *Life (Basel)* **2017**, *7*, 5.
12. Hargreaves, W.R., Mulvihill, S.J., Deamer, D.W. Synthesis of phospholipids and membranes in prebiotic conditions. *Nature* **1977**, *266*, 78–80.
13. Epps, D.E., Sherwood, E., Eichberg, J., Or, J. Cyanamide mediated syntheses under plausible primitive earth conditions: V. The Synthesis of Phosphatidic Acids. *J. Mol. Evol* **1978**, *11*, 279–292.
14. Epps, D.E., Noonan, D.W., Eichberg, J., Sherwood, E., Oró, J. Cyanamide mediated synthesis under plausible primitive earth conditions: VI. The Synthesis of Glycerol and Glycerophosphates. *J. Mol. Evol* **1979**, *14*, 235–241.
15. Rao, M., Eichberg, J., Oró, J. Synthesis of phosphatidylcholine under possible primitive Earth conditions. *J. Mol. Evol* **1982**, *18*, 196–202.
16. Rao, M., Eichberg, J., Oró, J. Synthesis of phosphatidylethanolamine under possible primitive earth conditions. *J. Mol. Evol* **1987**, *25*, 1–6.
17. Fiore, M. The synthesis of mono-alkyl phosphates and their derivatives: an overview of their nature, preparation and use, including synthesis under plausible prebiotic conditions. *Org. Biomol. Chem* **2018**, *16*, 3068–3086.
18. Tanford, C. The Hydrophobic Effect: Formation of Micelles and Biological Membranes. *Science*, **1973**.
19. Fiore, M., Madanamoothoo, W., Berlioz-Barbier, A., Maniti, O., Girard-Egrot, A., Buchet, R., Strazewski, P. Giant vesicles from rehydrated crude mixtures containing unexpected mixtures of amphiphiles formed under plausibly prebiotic conditions. *Org. Biomol. Chem* **2017**, *15*, 4231–4240.

20. Thomson, A.J., and Gray, H.B. Bio-inorganic Chemistry. *Curr Opin Chem Biol* **1998**, *2*, 155–158.
21. Sissi, C., and Palumbo, M. Effects of magnesium and related divalent metal ions in topoisomerase structure and function. *Nucleic Acids Res* **2009**, *37*, 702–711.
22. Fernandes, H.S., Teixeira, C.S.S., Sousa, S.F., Cerqueira, N.M.F.S.A, Formation of Unstable and very Reactive Chemical Species Catalyzed by Metalloenzymes: A Mechanistic Overview. *Molecules* **2019**, *24*, 2462.
23. Giles, N.M., Watts, A.B., Giles, G.I., Fry, F.H., Littlechild, J.A., Jacob, C. Metal and redox modulation of cysteine protein function. *Chem. Biol* **2003**, *10*, 677–693.
24. Sundberg, R.J., and Martin, R.B. Interactions of histidine and other imidazole derivatives with transition metal ions in chemical and biological systems. *Chem. Rev* **1974**, *74*, 471–517.
25. Zheng, H., Chruszcz, M., Lasota, P., Lebioda, L., Minor, W. Data mining of metal ion environments present in protein structures. *J. Inorg. Biochem* **2008**, *102*, 1765–1776.
26. Belmonte, L., and Mansy, S.S. Metal Catalysts and the Origin of Life. *Elements* **2016**, *12*, 413–418.
27. Zheng, H., Cooper, D.R., Porebski, P.J., Shabalin, I, G., Handing, K.B., Minor, W. CheckMyMetal: a macromolecular metal-binding validation tool. *Acta Crystallographica Section D Structural Biology* **2017**, *73*, 223-233.
28. Bhattacharya, P.K., and Samnani, P.B. Metal Ions in Biochemistry. CRC press: 2020.
29. Maret, W., and Vallee, B.L. Cobalt as Probe and Label of Proteins. *Methods in Enzymology, Academic Press* **1993**, *226*, 52-71.
30. Dobson, C.M., Ellison, G.B., Tuck, A.F., Vaida, V. Atmospheric aerosols as prebiotic chemical reactors. *PNAS* **2000**, *97*, 11864–11868.
31. Baeza, I., Ibañez, M., Santiago, J.C., Wong, C., Lazcano, A., OróStudies, J. Studies on protocellular evolution: the encapsulation of polyribonucleotides by liposomes. *Adv Space Res* **1986**, *6*, 39-43.
32. Woźniczka, M., Vogt, A., Kufelnicki, A. Equilibria in cobalt (II)-amino acid-imidazole system under oxygen-free conditions: effect of side groups on mixed-ligand systems with selected l- α -amino acids. *Chem Cent J* **2016**, *10*, 14.
33. National Library of Medicine. <https://pubchem.ncbi.nlm.nih.gov/>
34. Bhal, S.k. Log P-Making Sense of the Value. https://www.acdlabs.com/download/app/physchem/making_sense.pdf
35. Cheng, T., Zhao, Y., Li, X., Lin, F., Xu, Y., Zhang, X., Li, Y., Wang, R., Lai, L. Computation of octanol-water partition coefficients by guiding an additive model with knowledge. *J Chem Inf Model* **2007**, *47*, 2140-8.

Appendix

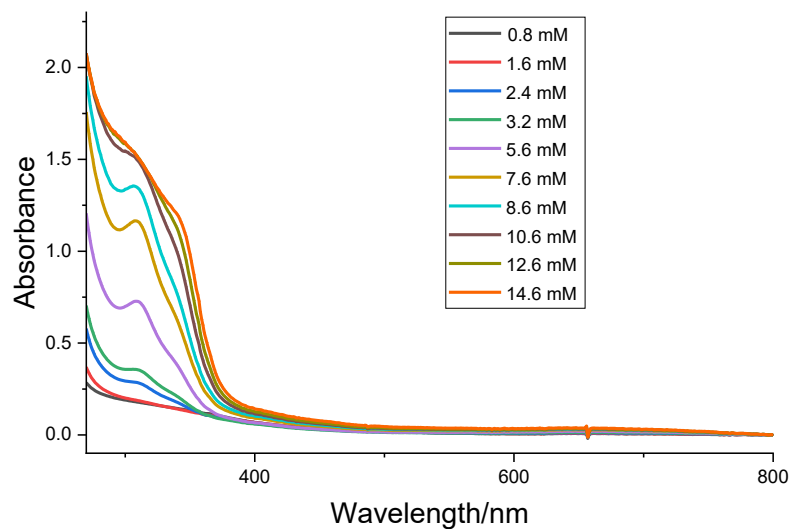


Figure A.1. The UV-Vis spectra of Iron titrations with N-Acetyl-L-cysteine methyl ester. 3 mM Fe (II) and 100 mM HEPBS, pH 8.8 was used.

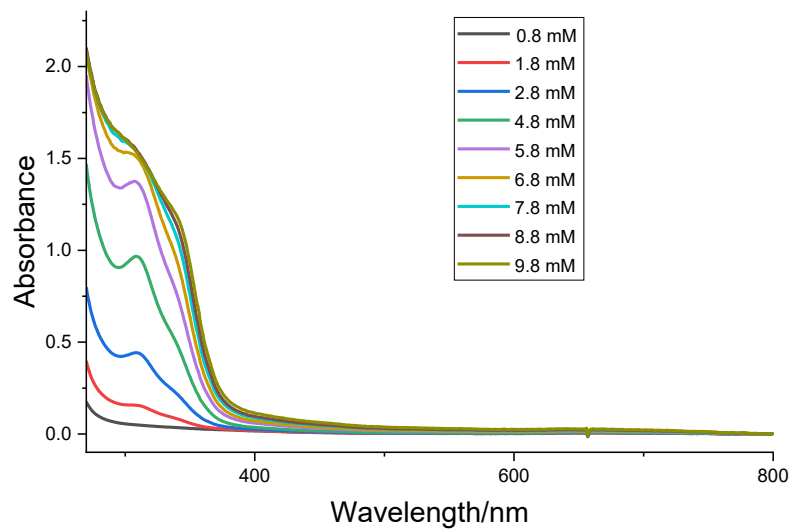


Figure A.2. The UV-Vis spectra of Iron titrations with N-Acetyl-L-cysteine methyl ester. 3 mM Fe (II) and 100 mM HEPBS, pH 8.8 was used.

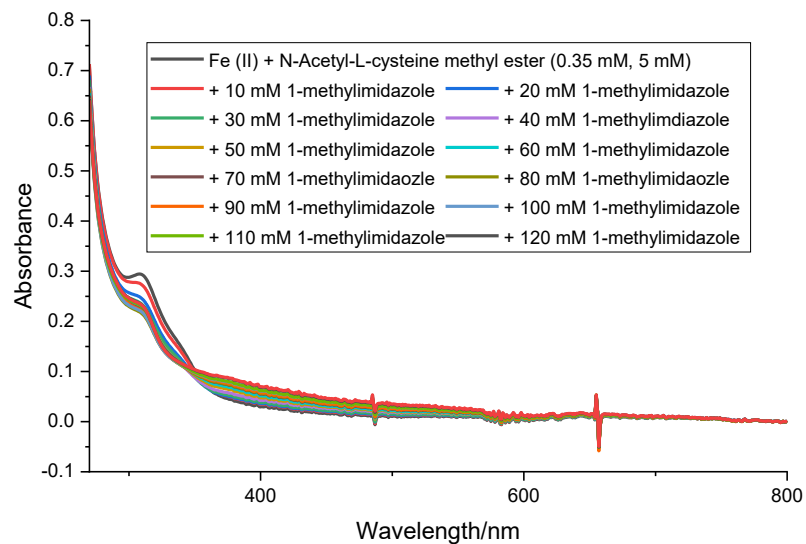


Figure A.3. The UV-Vis spectra of Fe (II)-N-Acetyl-L-cysteine methyl ester complex titrations with 1-methylimidazole. 0.35 mM Fe (II), 5 mM N-Acetyl-L-cysteine methyl ester, 100 mM HEPBS, pH 8.8 was used.

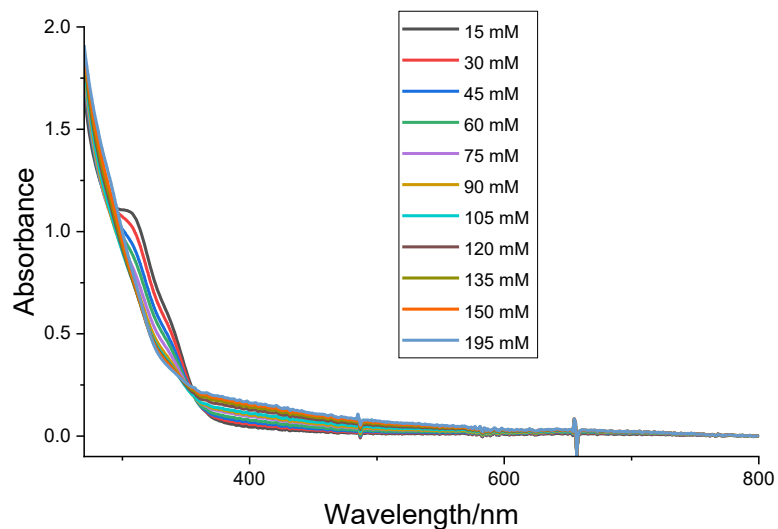


Figure A.4. The UV-Vis spectra of Fe (II)-N-Acetyl-L-cysteine methyl ester complex titrations with 1-butylimidazole. 0.35 mM Fe (II), 5 mM N-Acetyl-L-cysteine methyl ester, 100 mM HEPBS, pH 8.8 was used.